Supplementary materials

Zn(II) and Co(II) coordination polymers based on semi-rigid bis-pyridyl-bis-amide and angular dicarboxylate ligands: synthesis, structures and properties

Venkatesan Lakshmanan,[a] Chia-Yi Lee,[a] Yu-Wen Tseng,[a]

Yu-Hsiang Liu,[a] Chia-Her Lin[b,*] and Jhy-Der Chen[a,*]

[1] Department of Chemistry, Chung-Yuan Christian University, Taoyuan City, 320, Taiwan R. O. C;

[2] Department of Chemistry, National Taiwan Normal University, Taipei, Taiwan, R. O. C.

Scheme S1 Structures of selected pesticides.

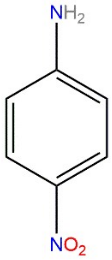

4-NA

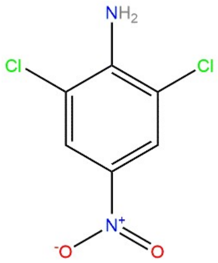

2,6-DCNA

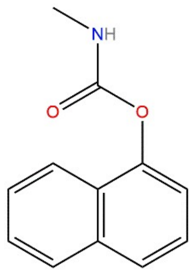

Carbaryl

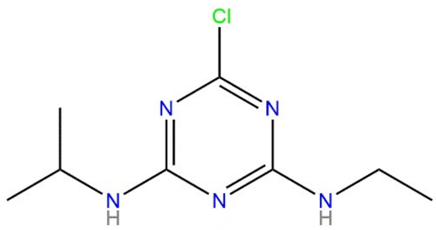

Atrazine

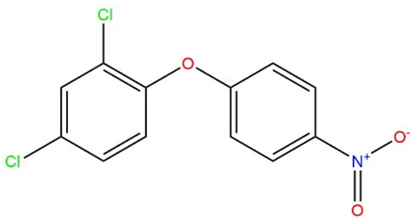

Nitrofen

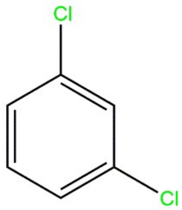

1,3-Dichlorobenzene

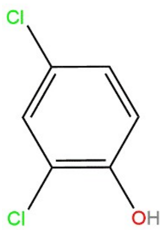

2,4-Dichlorophenol

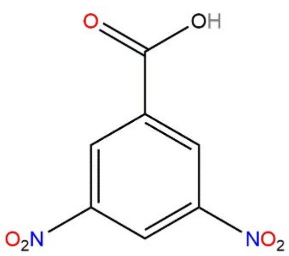

3,5-Dinitrobenzoic acid

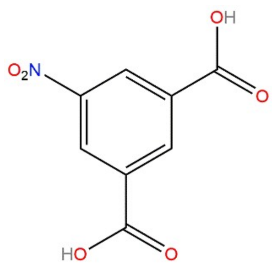

5-Nitroisophthalic acid

Fig. S1 FT-IR spectra of complexes (a) **1** (b) **2** (c) **3** (d) **4** (e) **5** and (f) **6**.

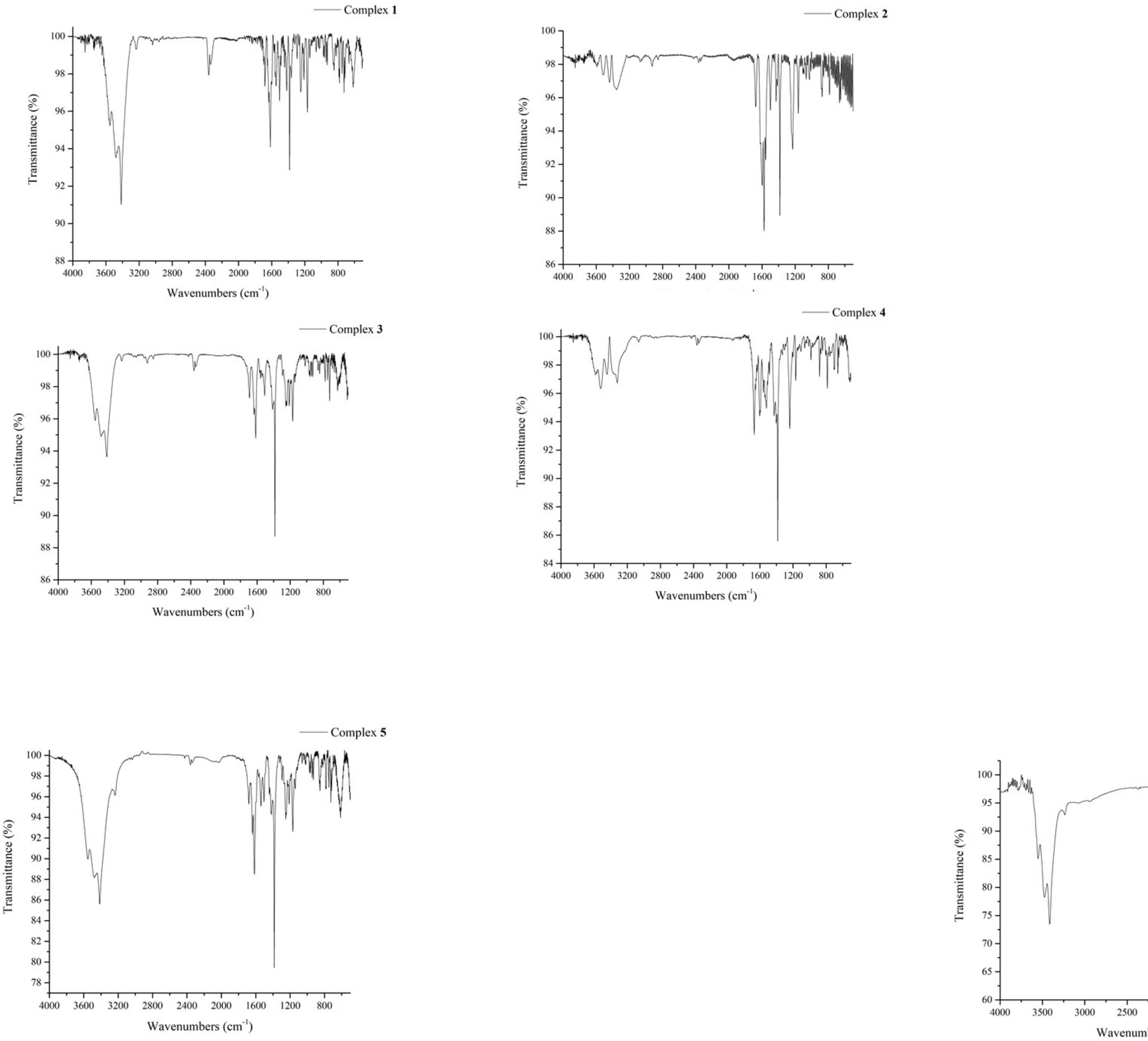

Fig. S2 (a) Simulated and (b) as synthesized PXRD patterns of complex **1**.

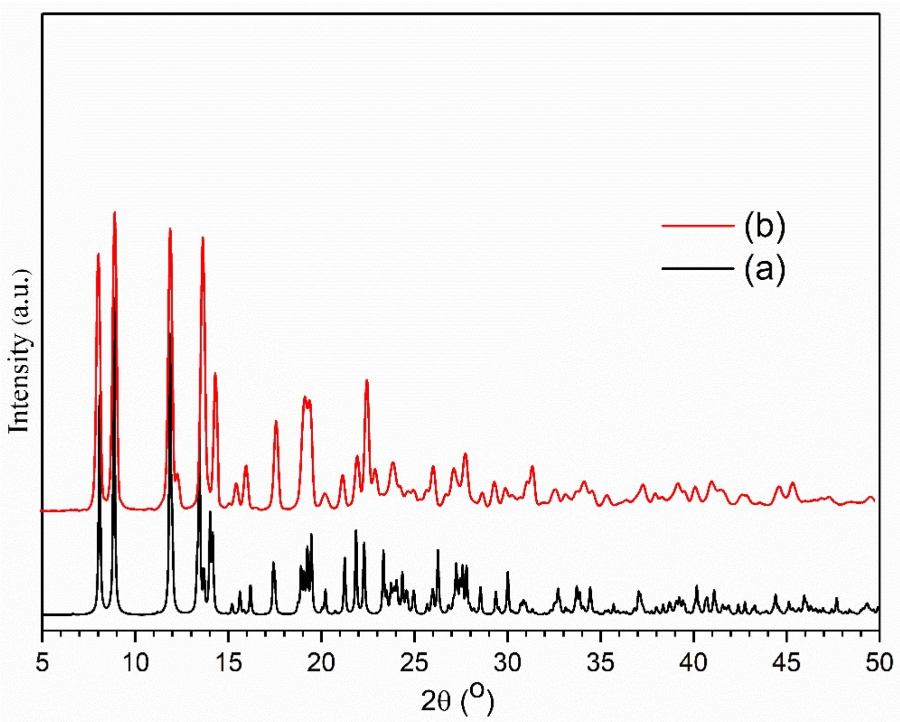

Fig. S3 (a) Simulated and (b) as synthesized PXRD patterns of complex **2**.

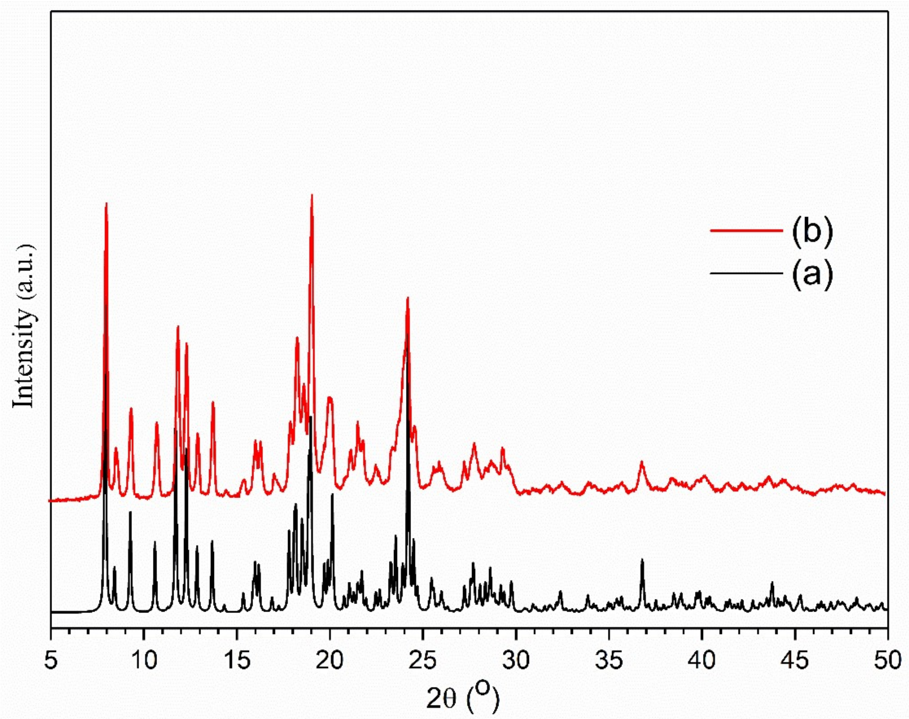

Fig. S4 (a) Simulated and (b) as synthesized PXRD patterns of complex **3**.

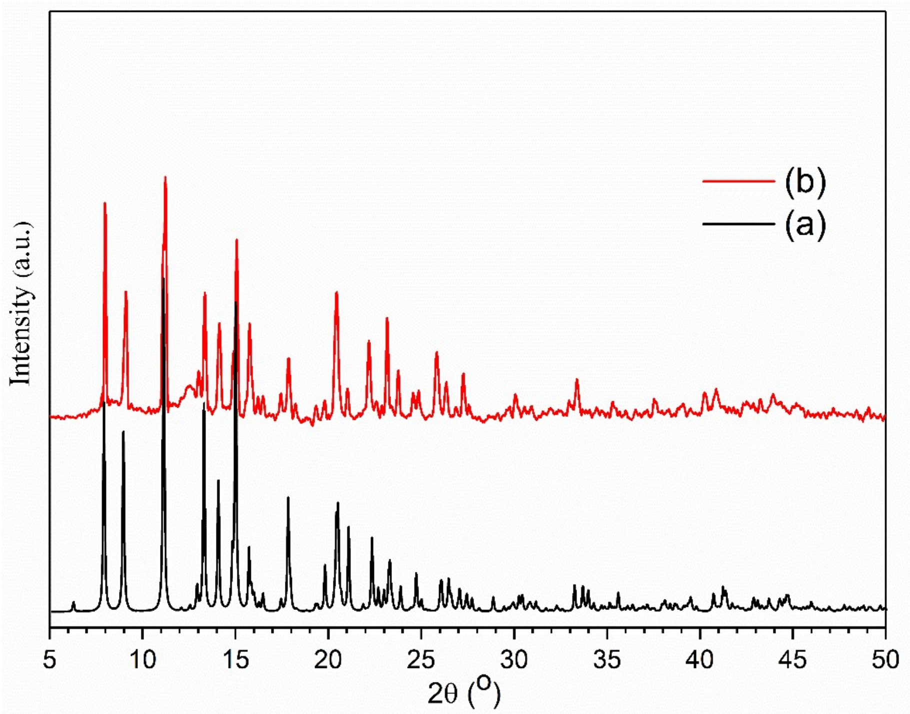

Fig. S5 (a) Simulated and (b) as synthesized PXRD patterns of complex **4**.

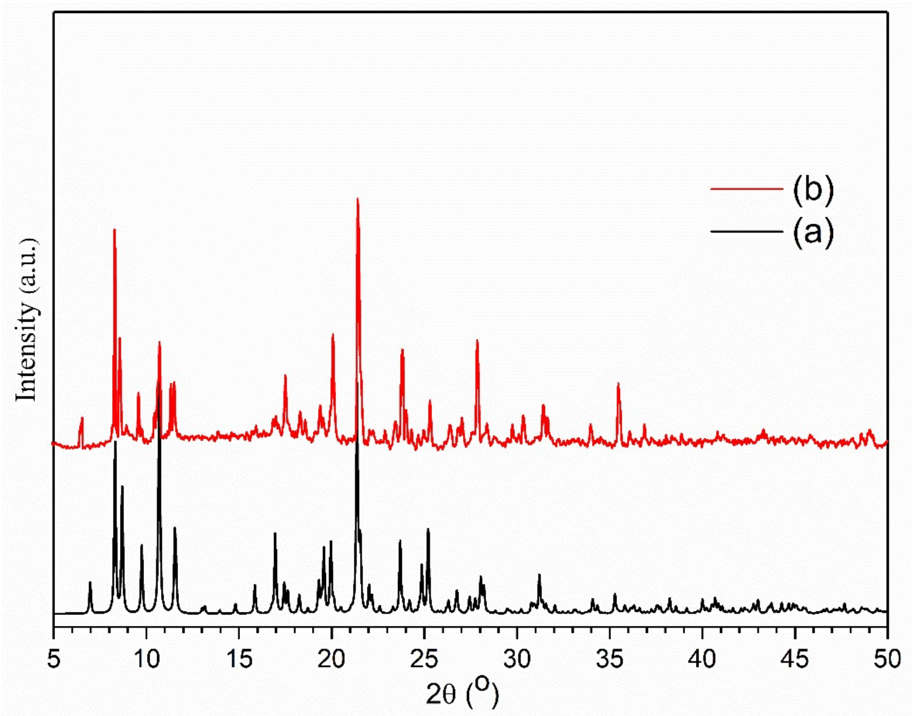

Fig. S6 (a) Simulated and (b) as synthesized PXRD patterns of complex **5**.

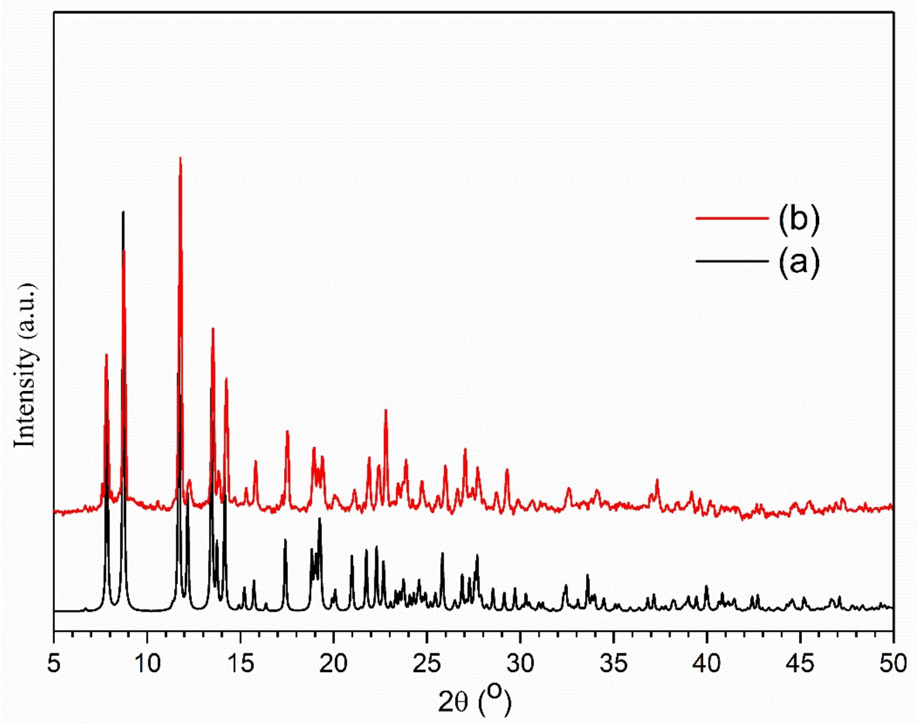

Fig. S7 (a) Simulated and (b) as synthesized PXRD patterns of complex **6**.

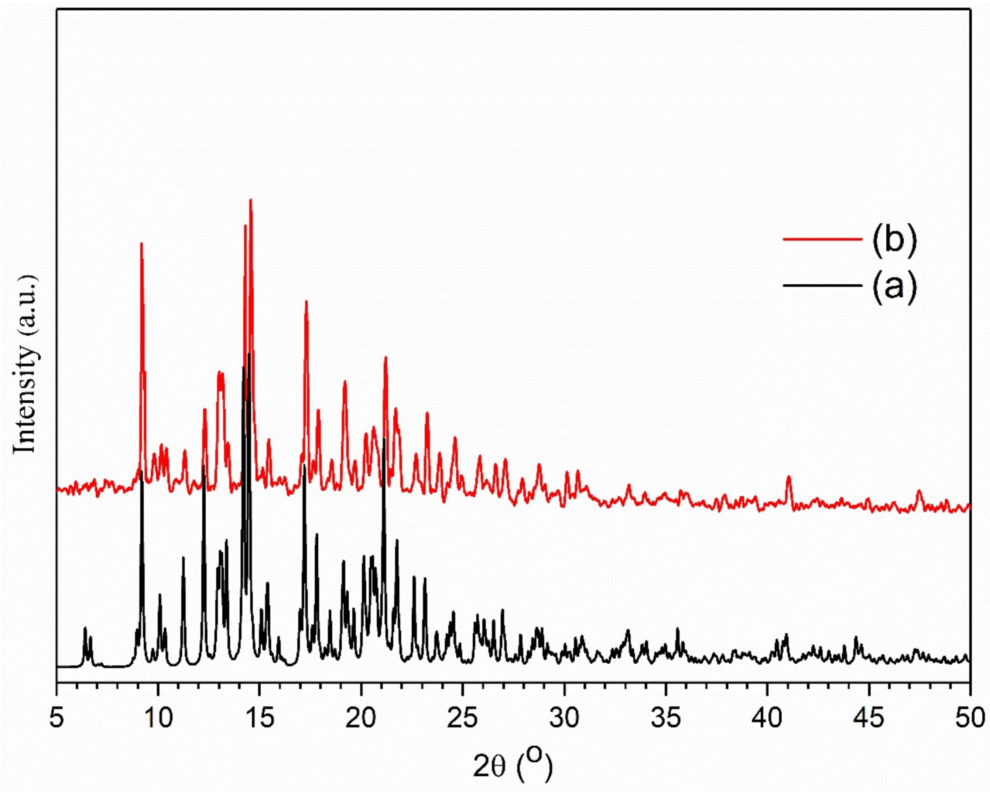

Fig. S8 TGA curves for complexes (a) **1** (b) **2** (c) **3** (d) **4** (e) **5** and (f) **6**.

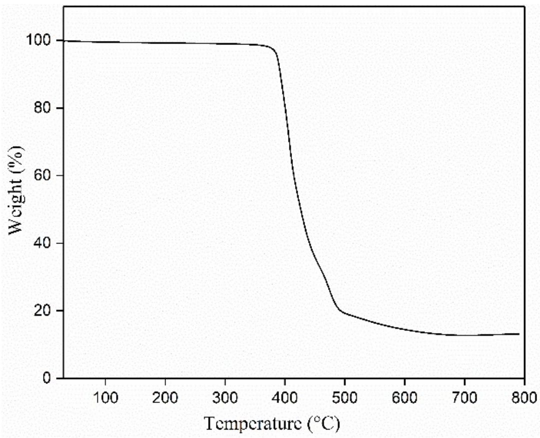

(a)

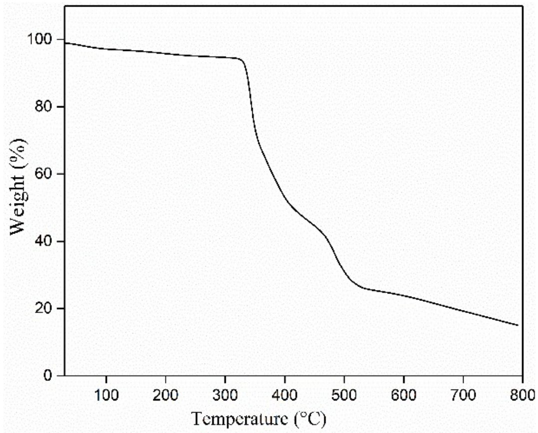

(b)

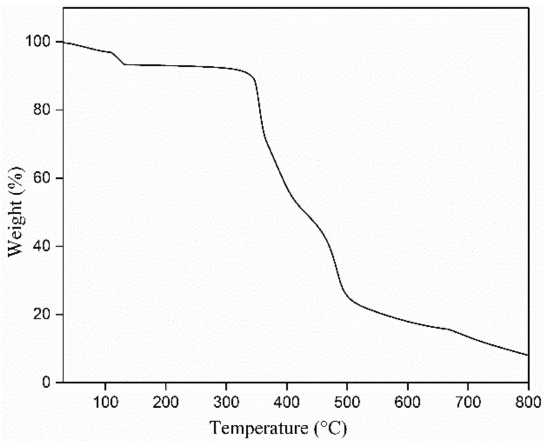

(c)

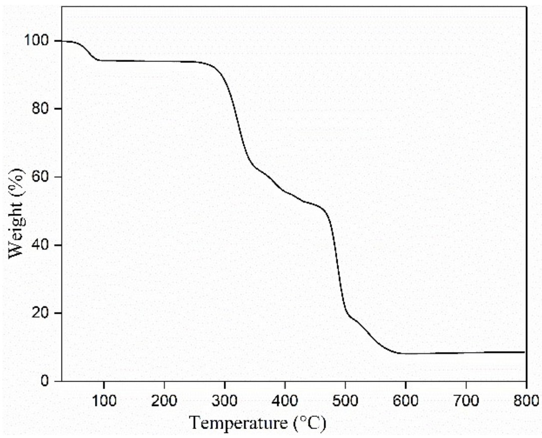

(d)

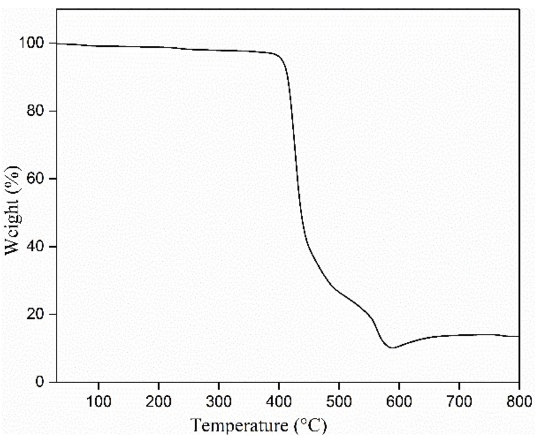

(e)

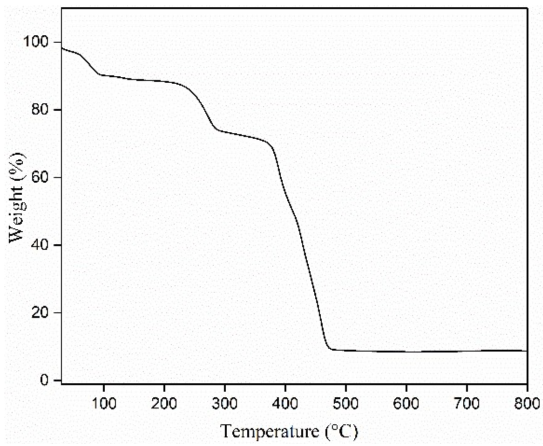

(f)

Fig. S9 IR spectra for the structural transformations from **6** to **5**. (a) CP **6**, (b) CP **6** in hydrothermal reaction. The IR spectrum was measured using the purple crystals collected, and (c) CP**5**.

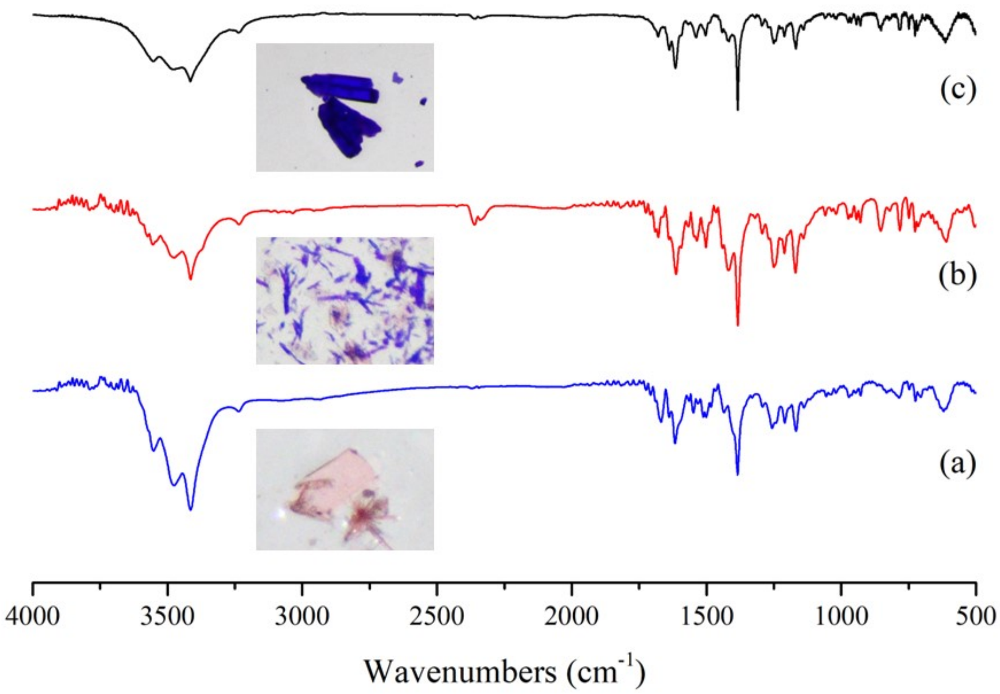

Fig. S10 PXRD patterns for transformation from **5** to **6**.

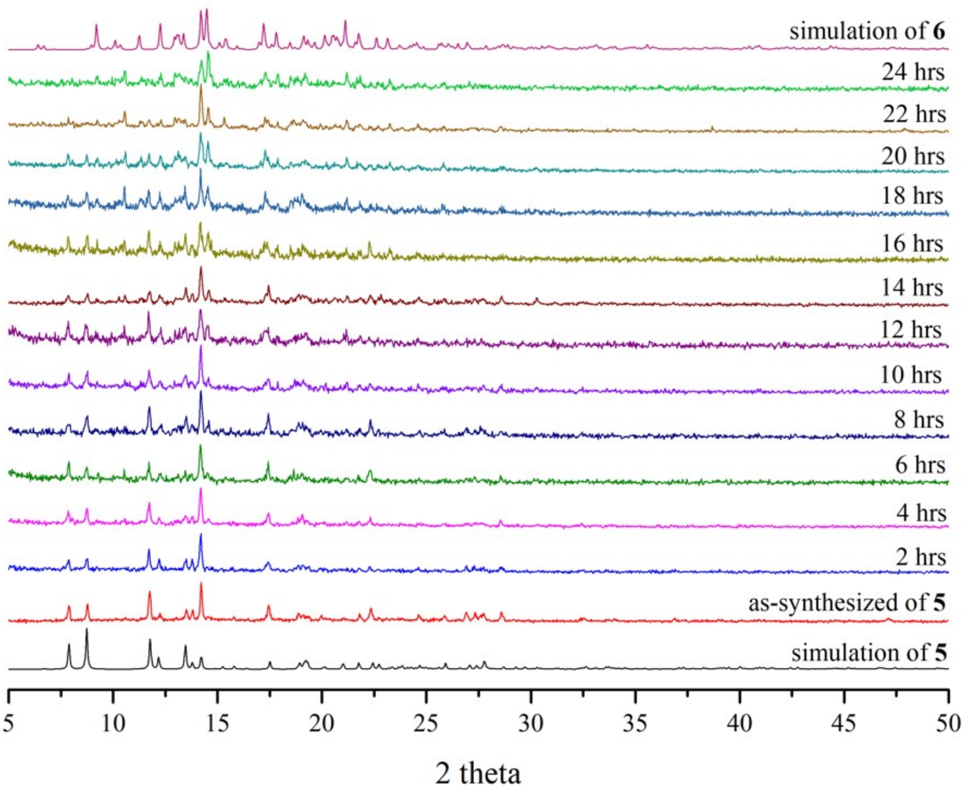

Fig. S11 IR spectra for the structural transformations from **5** to **6**. (a) CP **5**, (b) CP **5** in water at room temperature and (c) CP **6**.

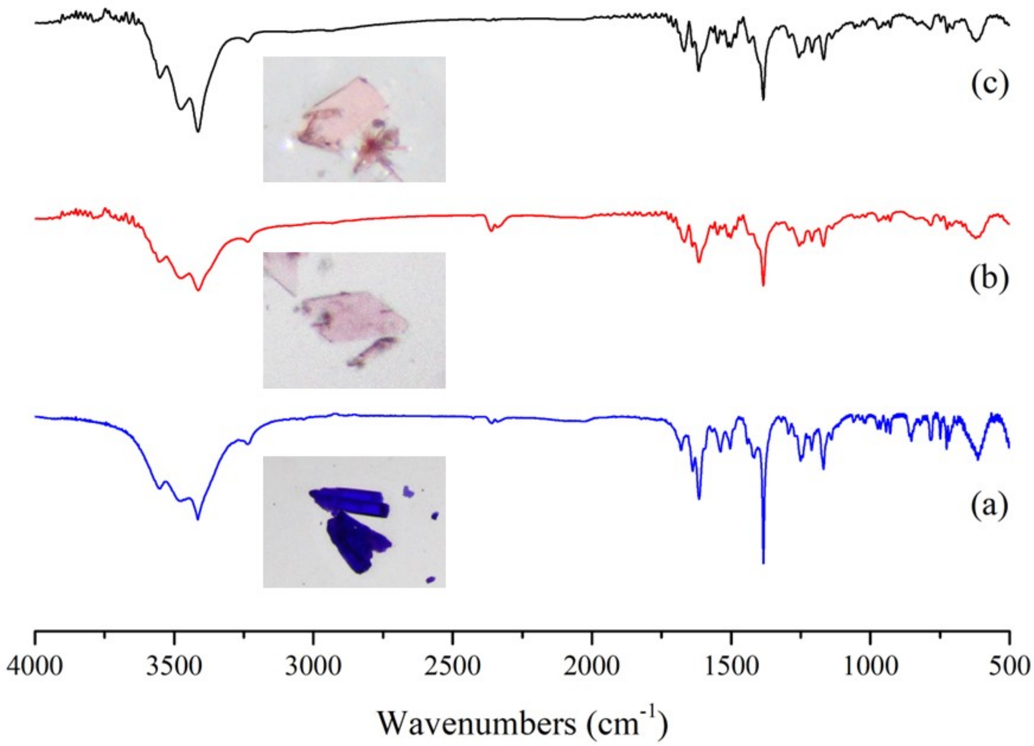

Fig. S12 PXRD patterns of the dehydrated and rehydrated (a) **1** and (b) **2,** and **1** and **2** immersed in solutions with various pH values.

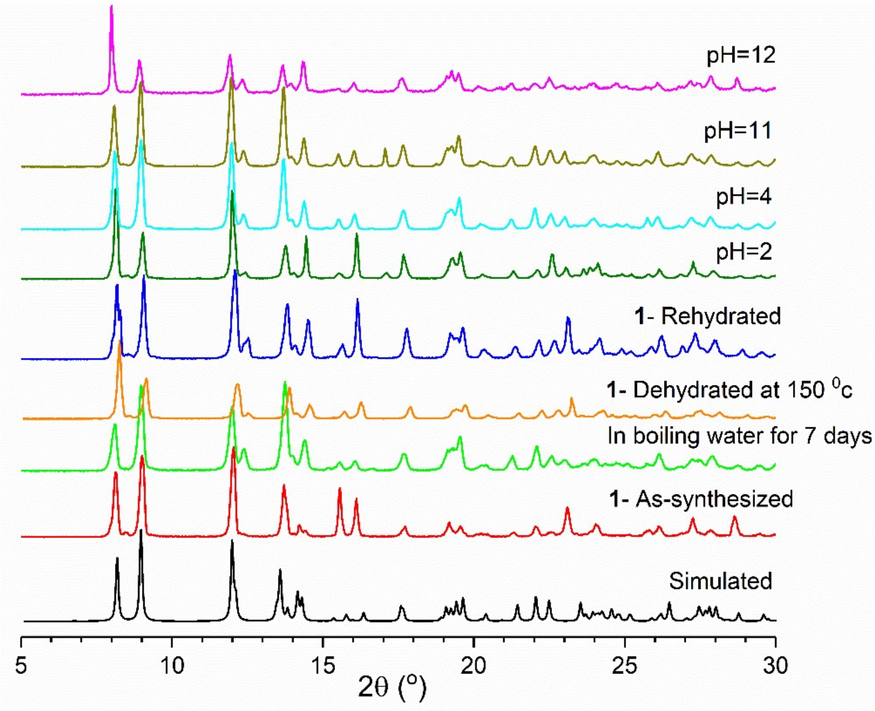

(a)

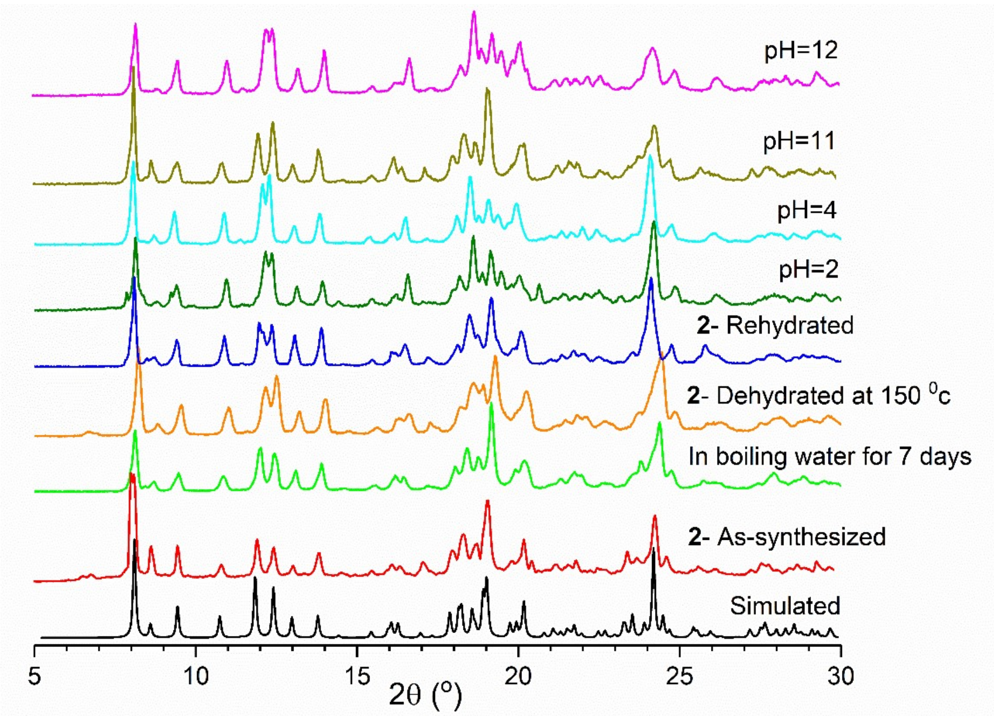

(b)

Fig. S13 PXRD patterns of (a) **1** and (b) **2** immersed in various solvents for 48 h.

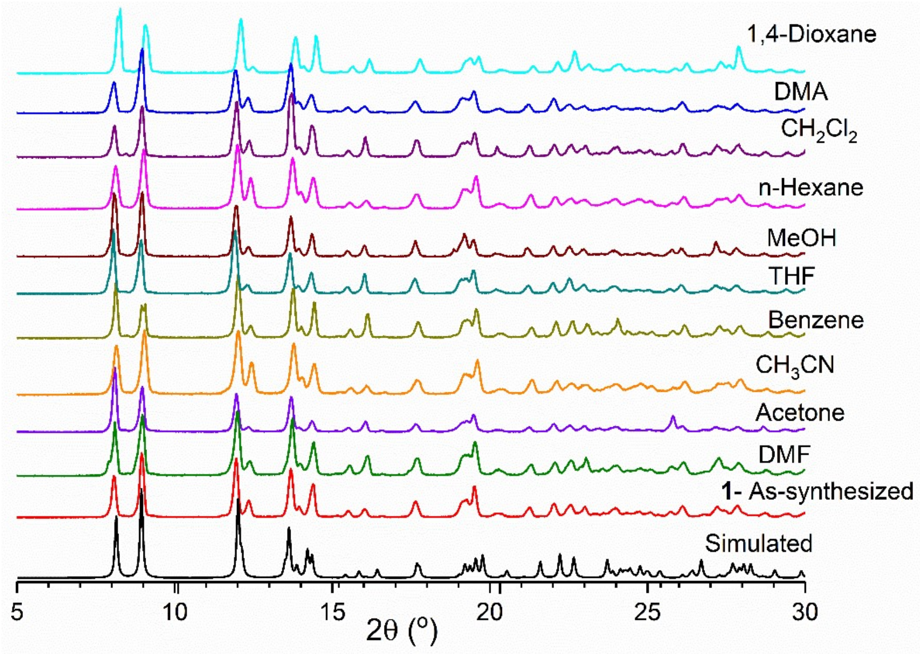

(a)

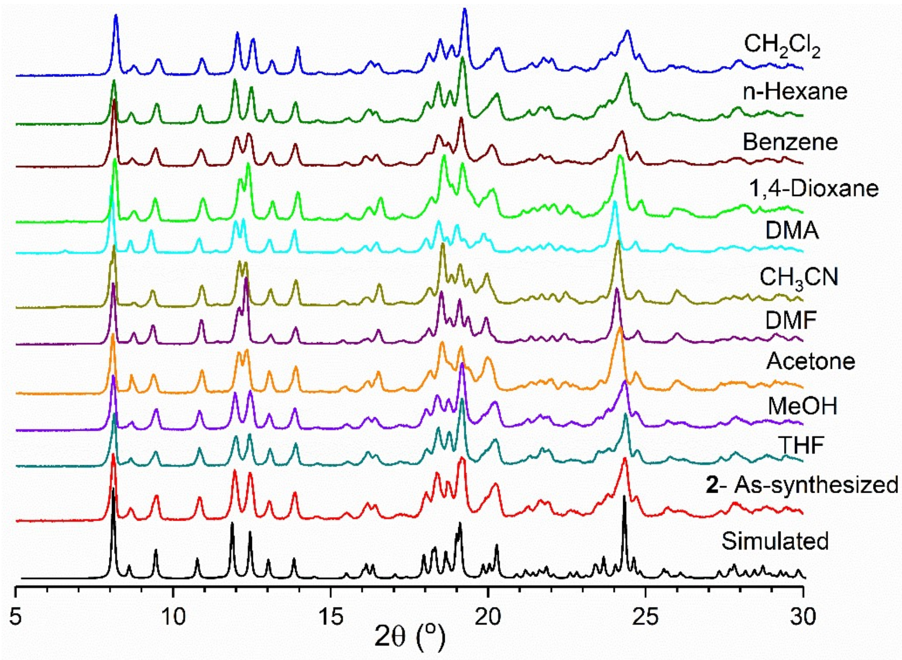

(b)

Fig. S14 (a) CO_2 sorption isotherm of complex **1** at 273 K and (b) pore size distributions.

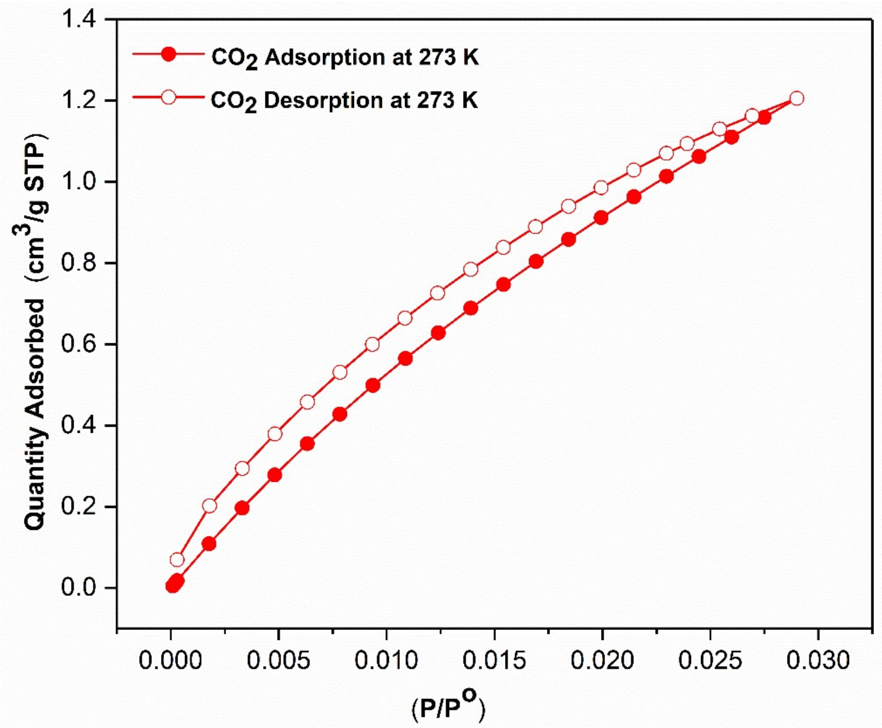

(a)

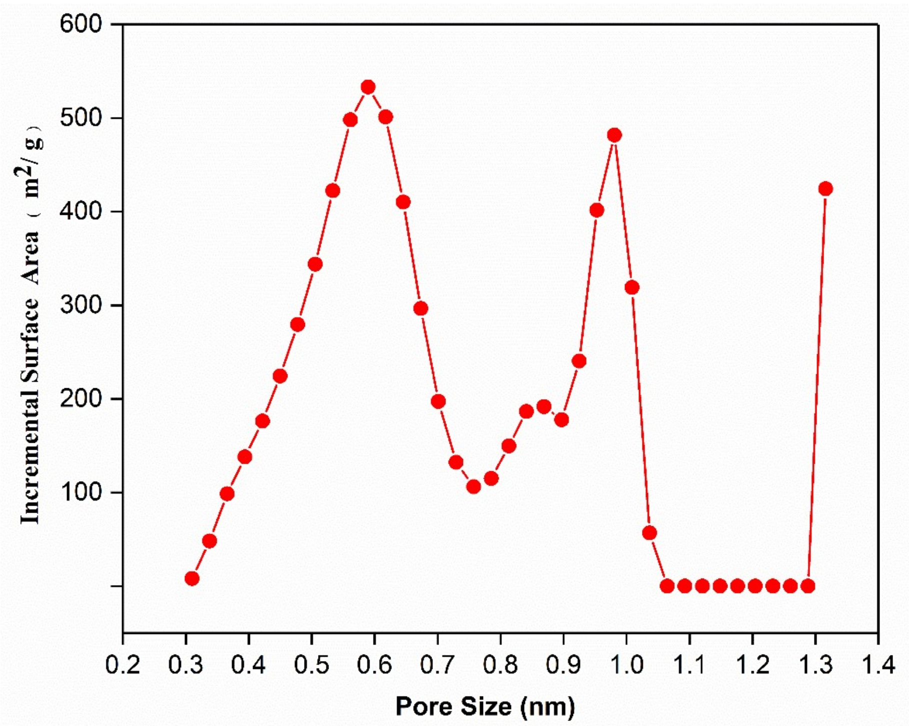

(b)

Fig. S15 (a) CO_2 sorption isotherm of complex **2** at 273 K and (b) pore size distributions.

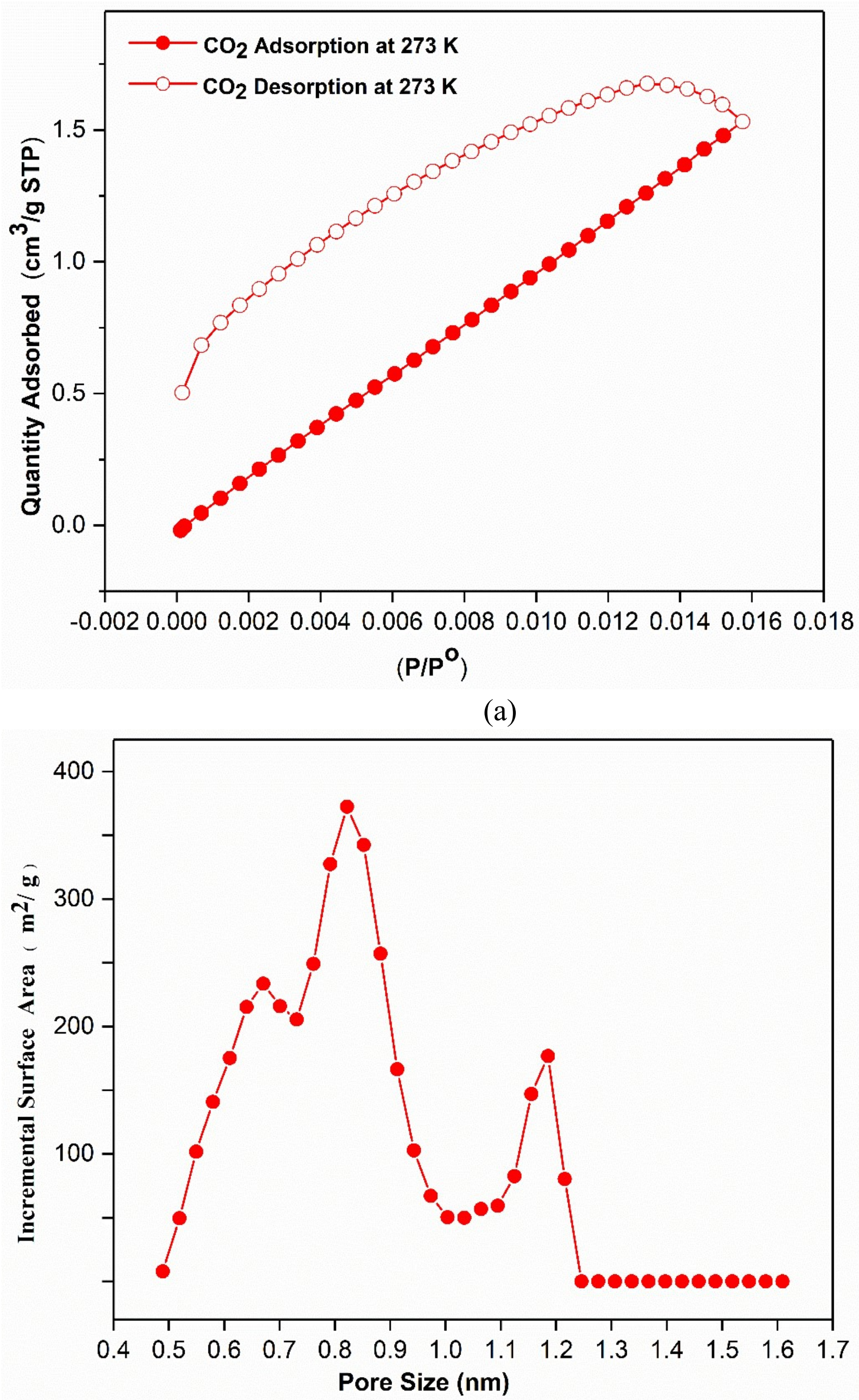

(a)

(b)

Fig. S16 CO_2 sorption isotherms of complexes (a) **1** and (b) **2** at 298 K and PXRD patterns of (c) **1** and (d) **2** measured after experiments.

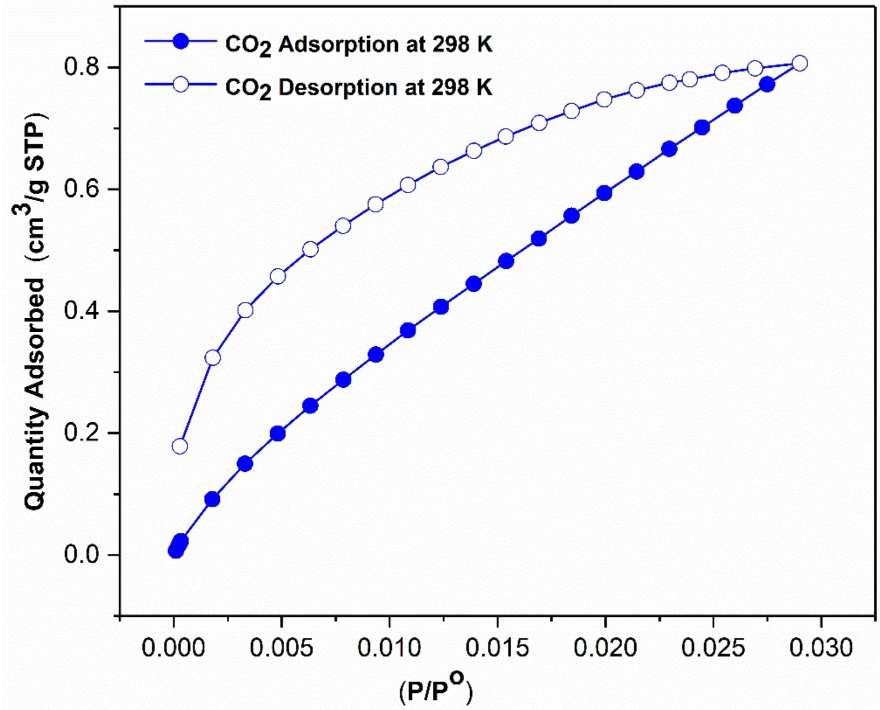

(a)

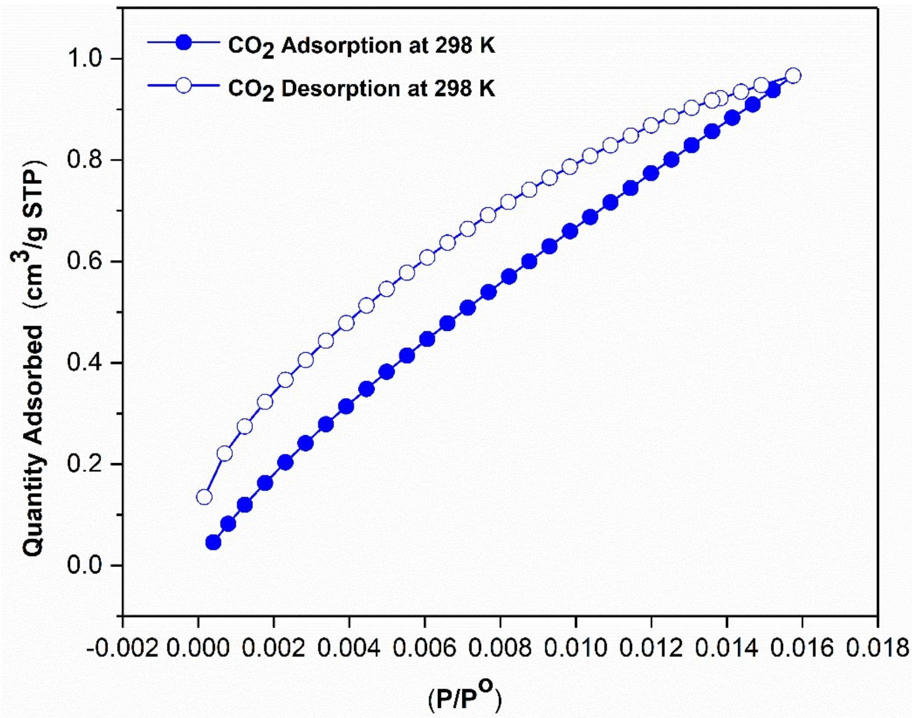

(b)

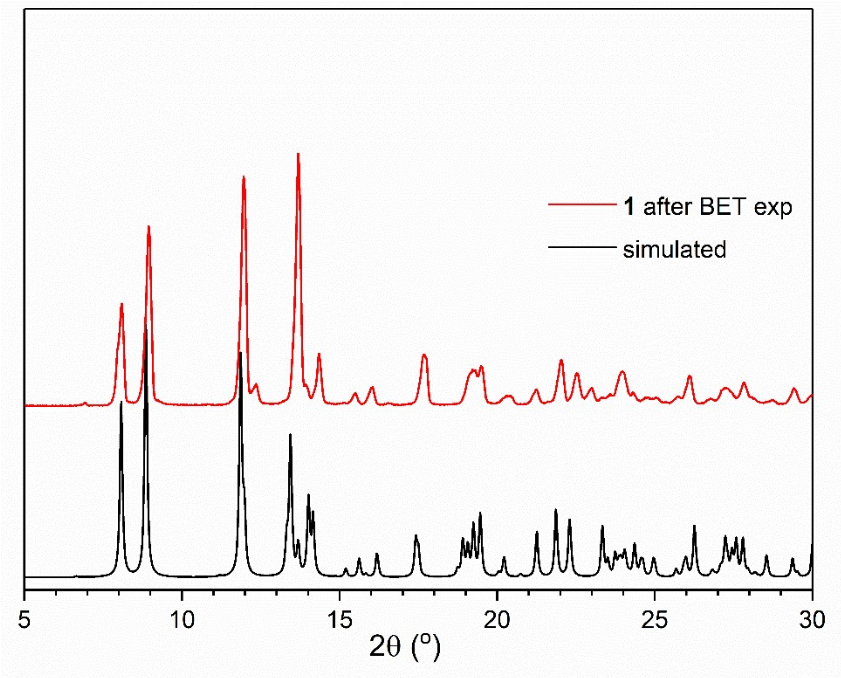
1 after BET exp
simulated
5
10
15
20
25
30
2θ (°)

(c)

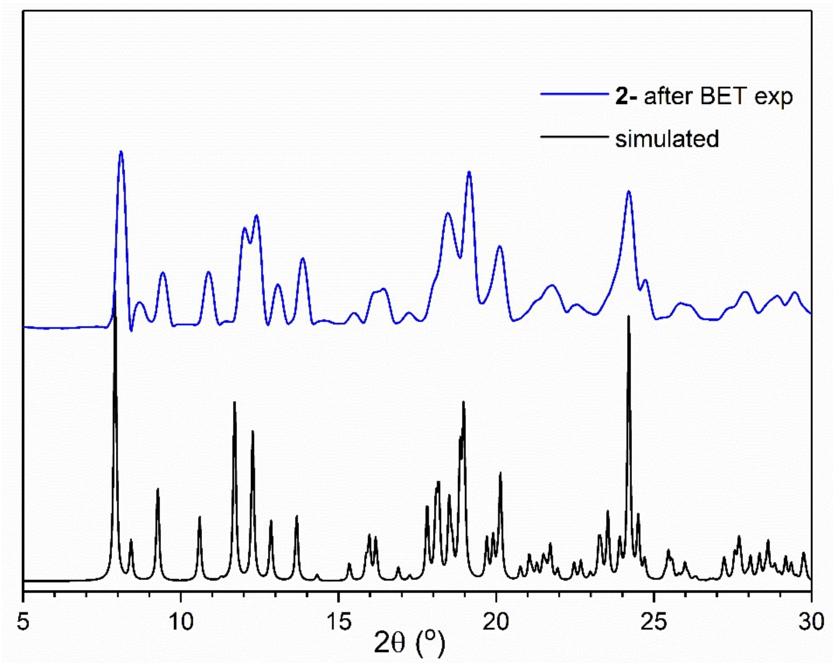
2- after BET exp
simulated
5
10
15
20
25
30
2θ (°)

(d)

Fig. S17 Excitation and emission spectra for (a) **L**[1] and **L**[2] and (b) H_2FIPBB, H_2OBA and **1** and **2**.

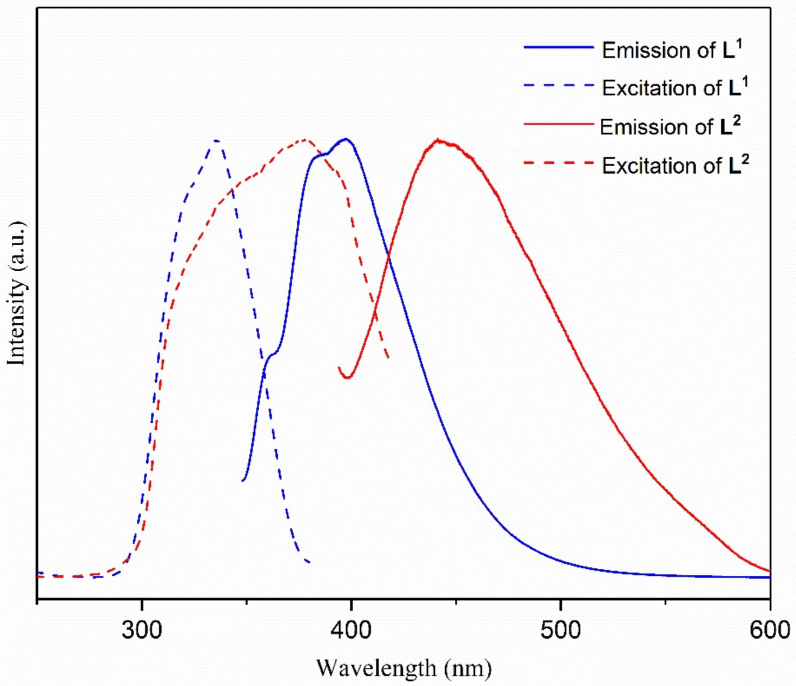

(a)

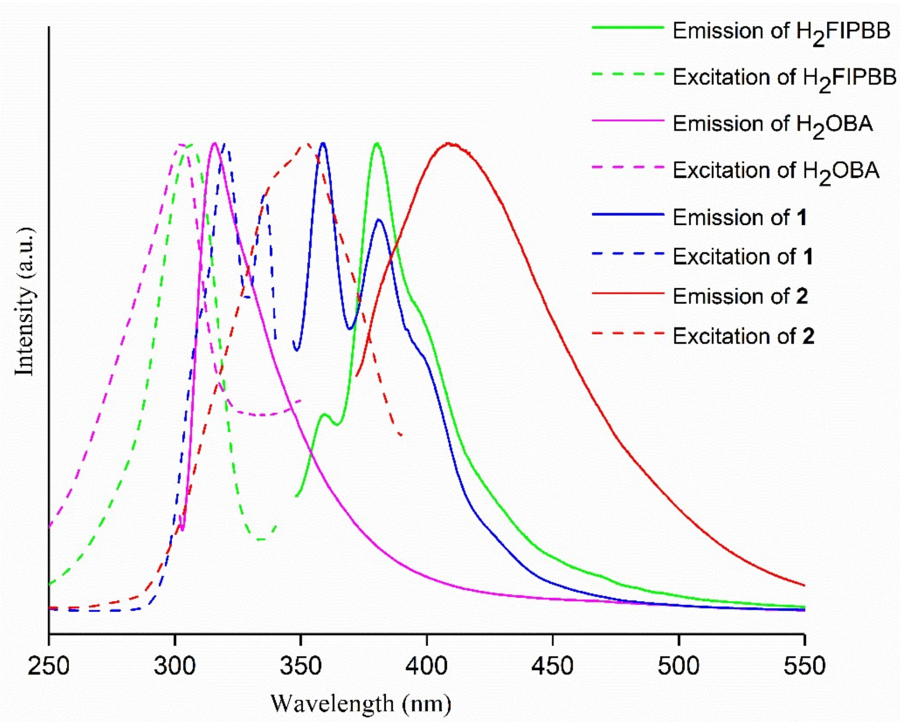

(b)

Fig. S18 Emission spectra of solvent-free (a) **1** and (b) **2** dispersed in DCM with various pesticides.

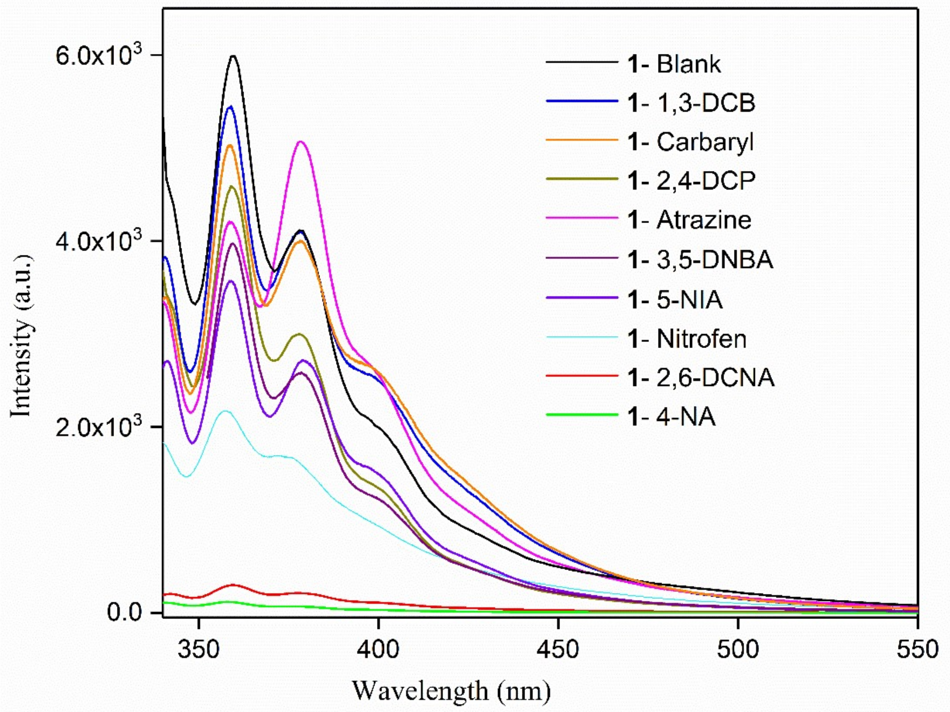

(a)

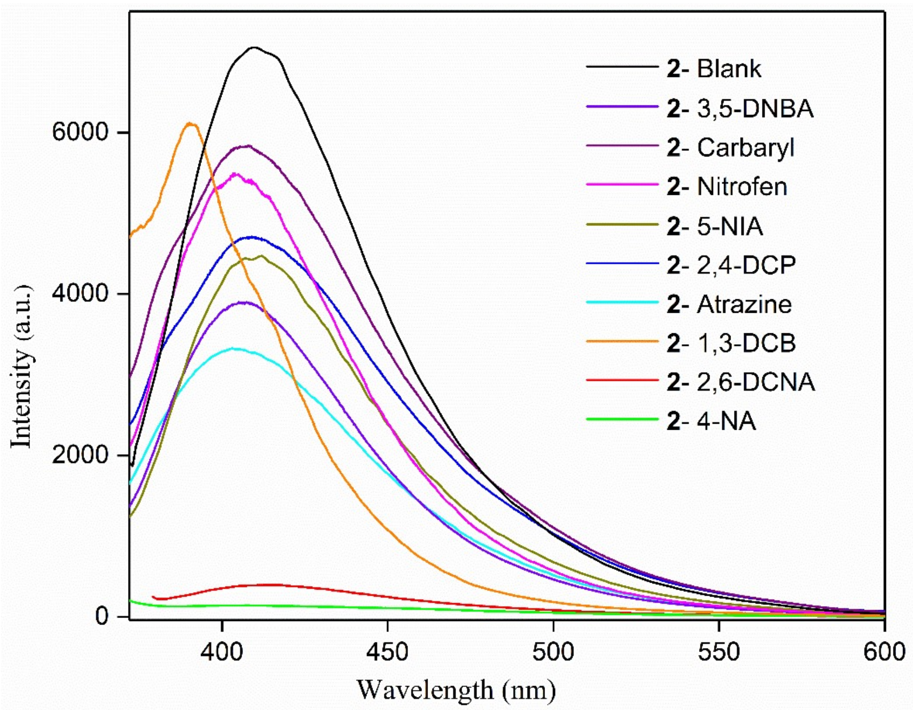

(b)

Fig. S19 PXRD patterns before and after treatments with 2,6-DCNA and 4-NA for (a) **1** and (b) **2**.

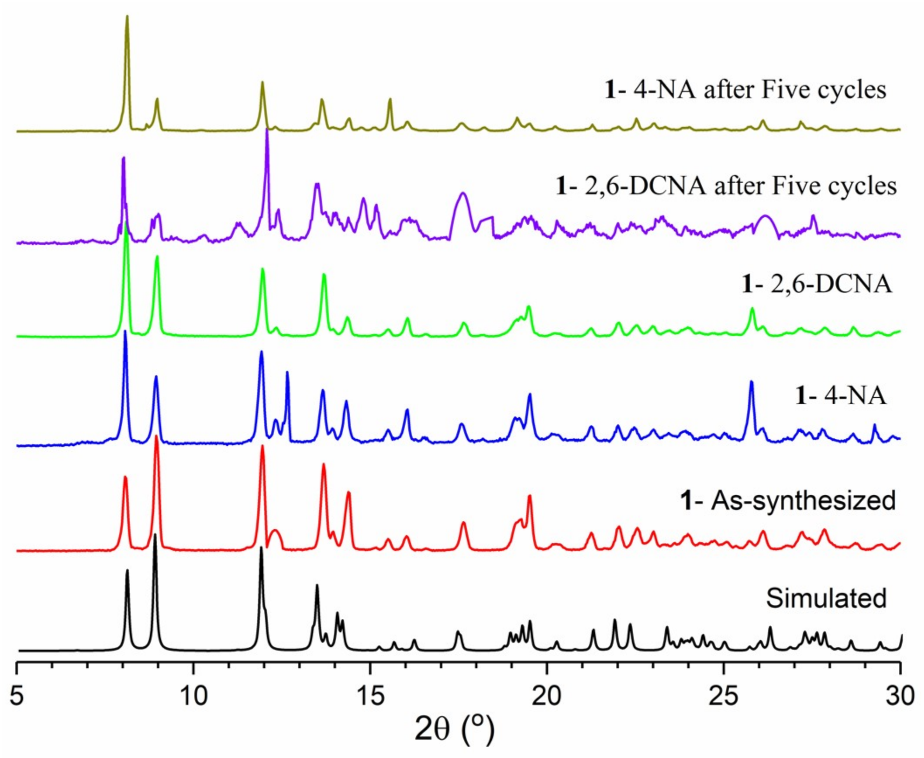

(a)

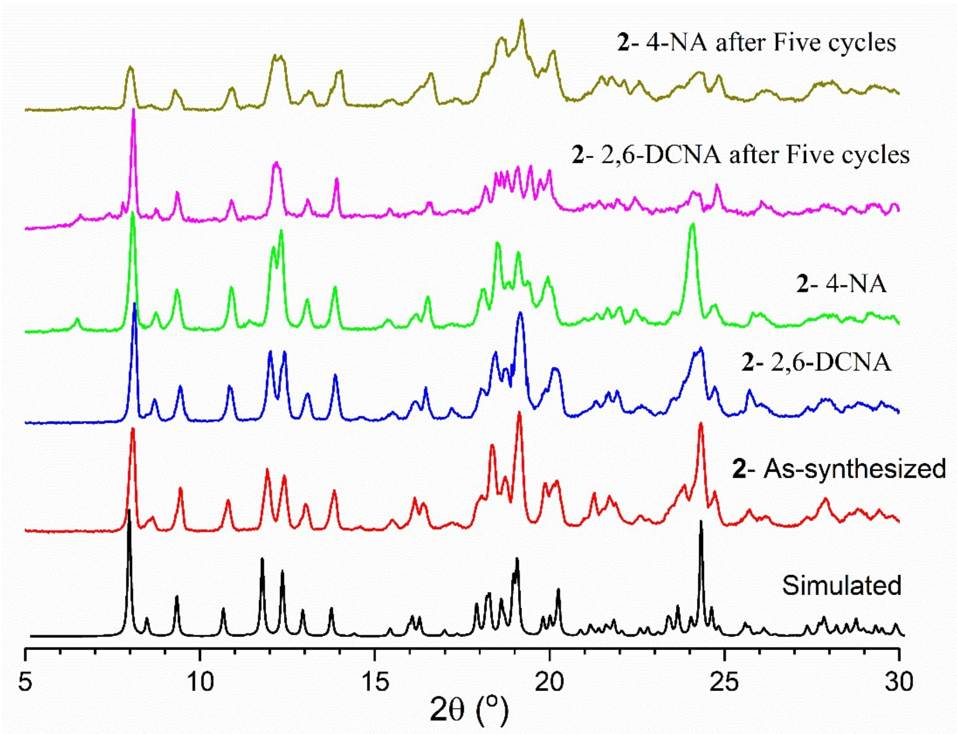

(b)

Fig. S20 Emission spectra of the activated samples **1** dispersed in DCM of (a) 2,6-DCNA and (b) 4-NA at various concentration.

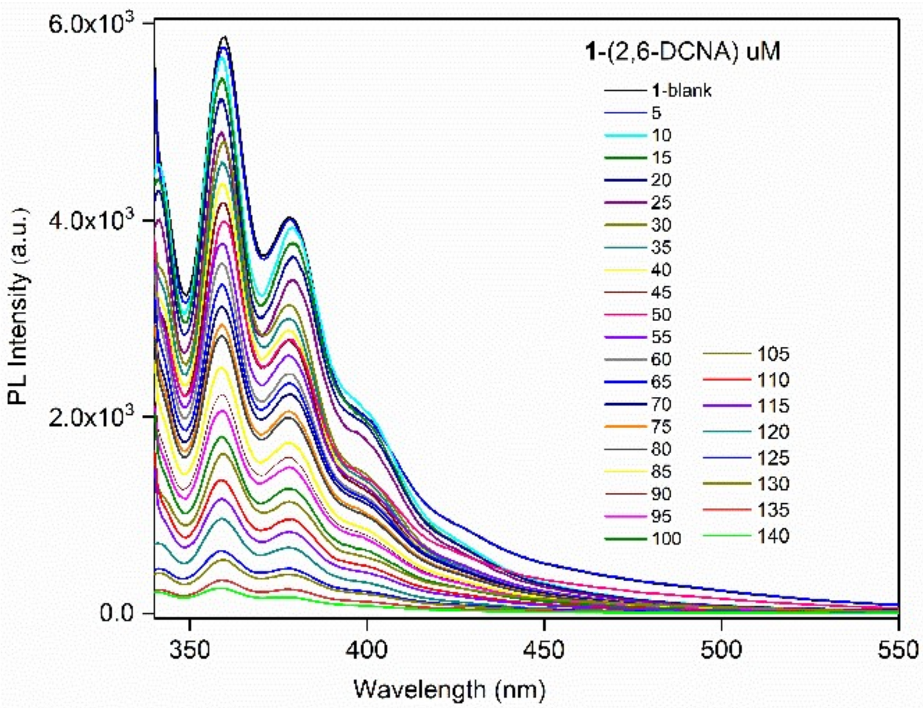

(a)

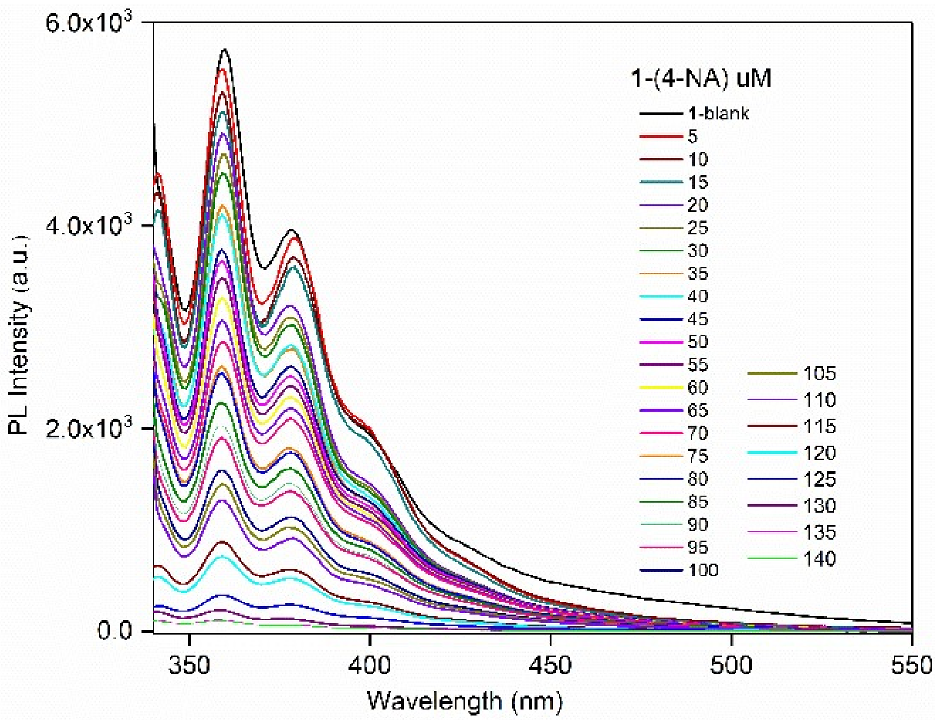

(b)

Fig. S21 Emission spectra of the activated samples **2** dispersed in DCM of (a) 2,6-DCNA and (b) 4-NA at various concentration.

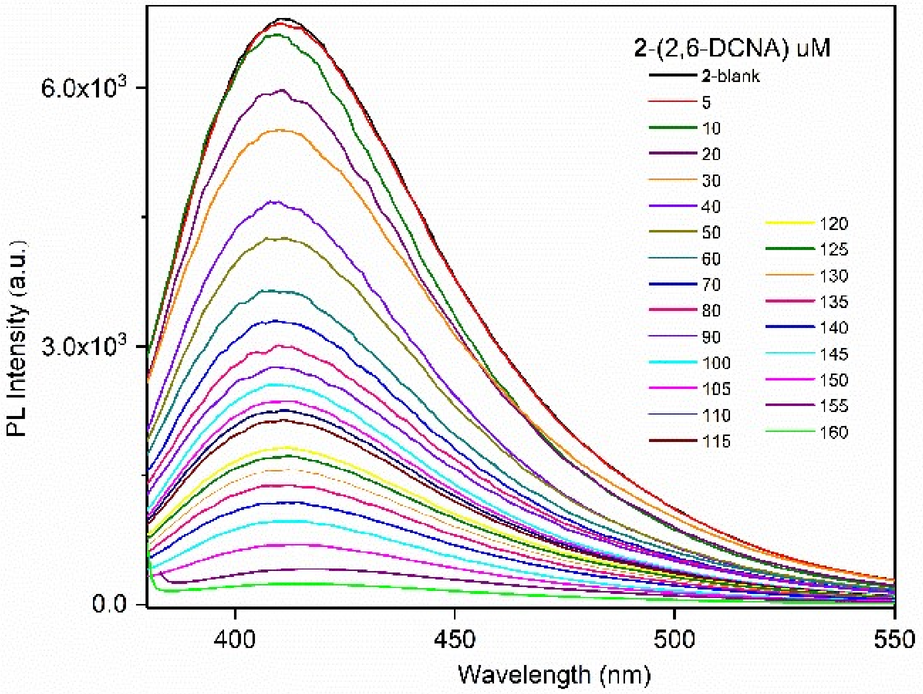

(a)

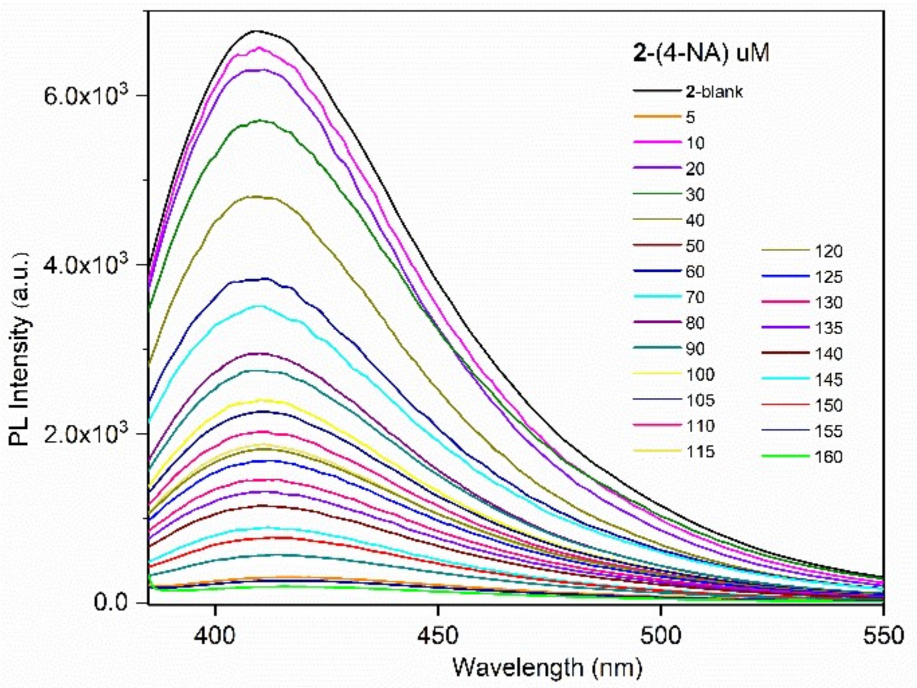

(b)

Fig. S22 (a) Bar diagrams showing the relative emission intensities of **1** and **2** dispersed in various pesticides and the Stern−Volmer (SV) plot of **1** in (b) 2,6-DCNA and (c) 4-NA and **2** in (d) 2,6-DCNA and (e) 4-NA, showing I_0/I versus analyte concentration.

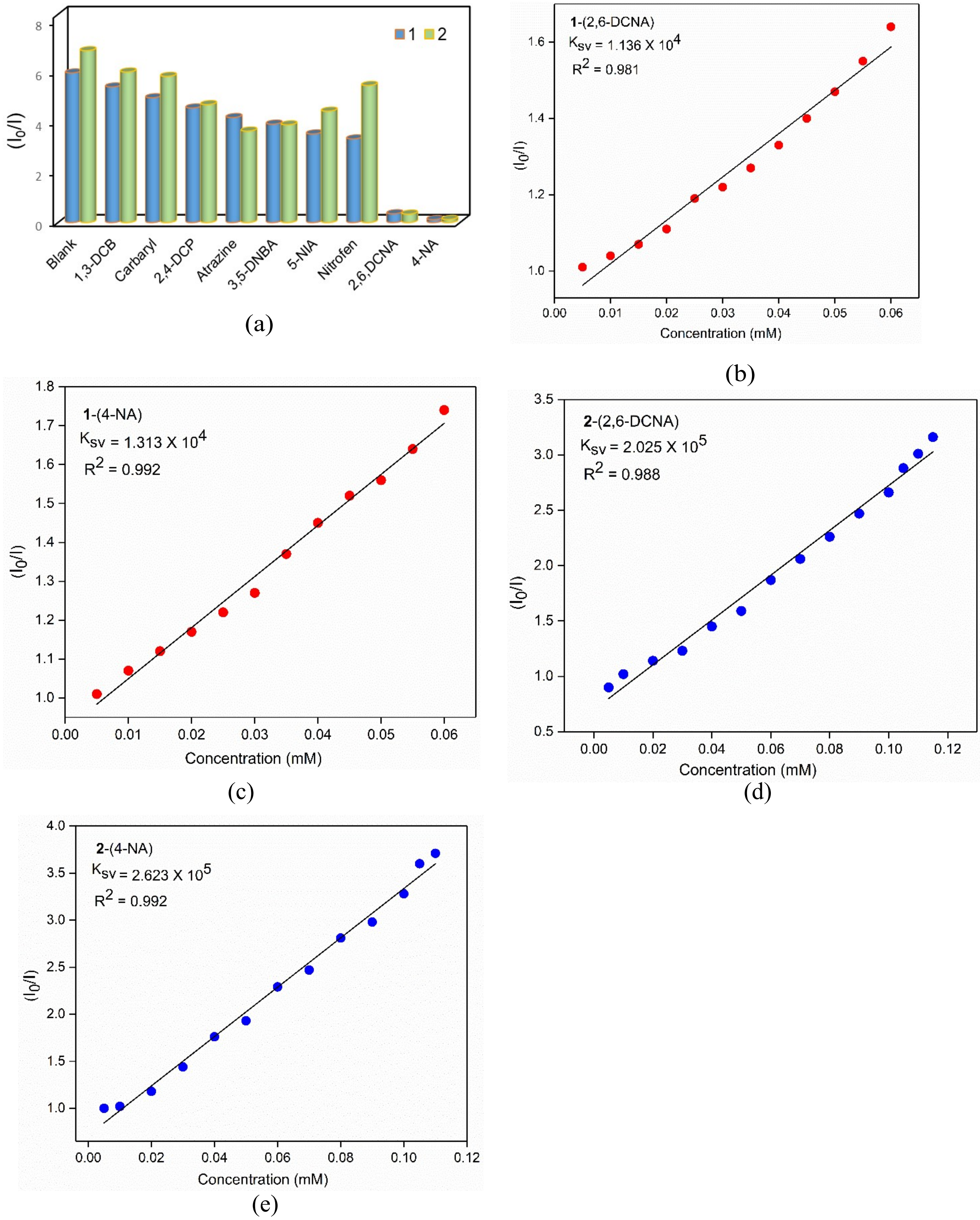

Fig. S23 Bar diagrams showing the emission intensities of (a) **1** and (b) **2** treated with 2,6-DCNA and 4-NA for five repeated cycles.

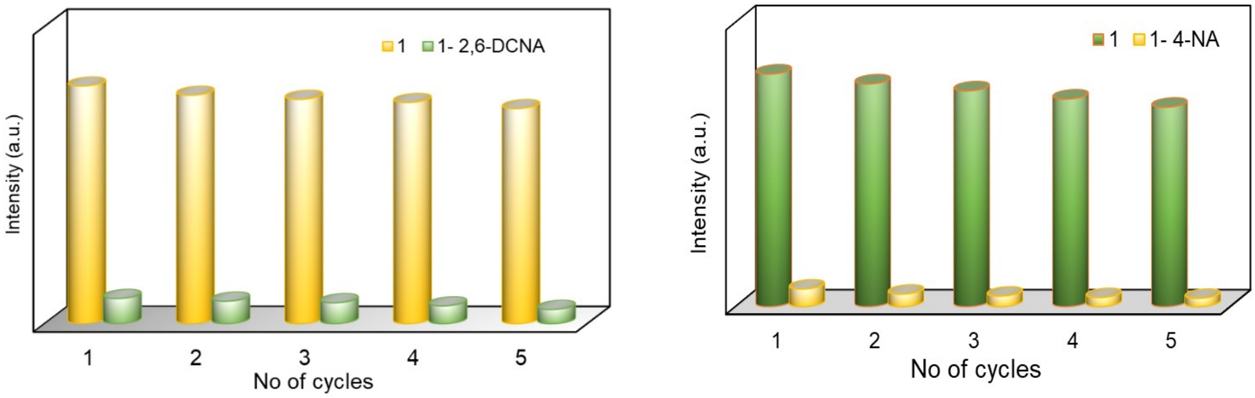

(a)

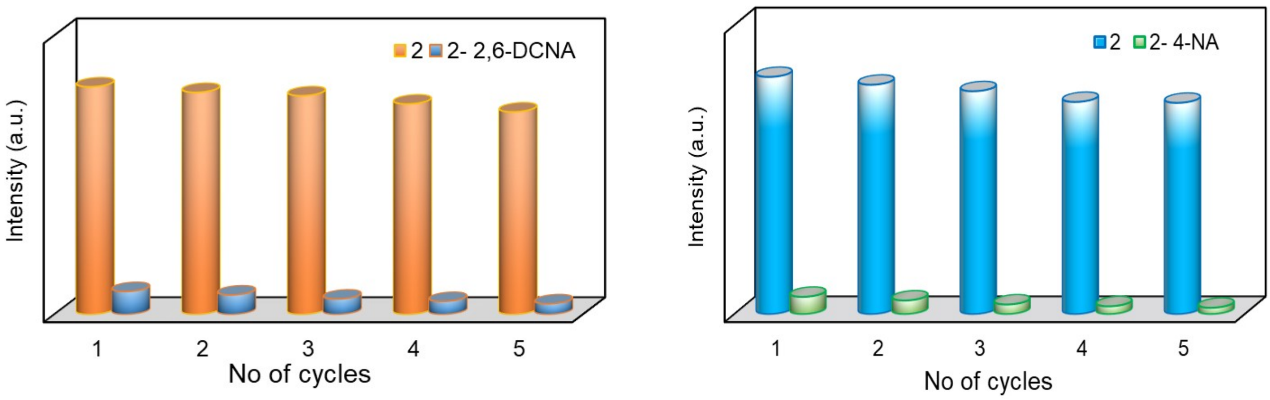

(b)

Fig. S24 The IR spectra of complex (a) **1** and (b) **2** before and after treated with 4-NA and 2,6-DCNA.

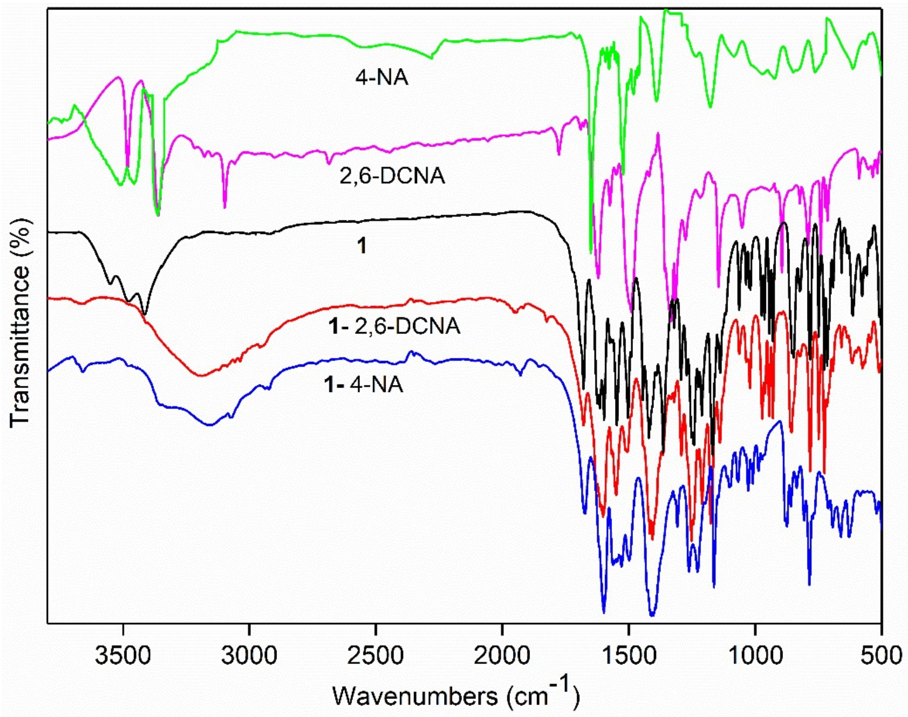

(a)

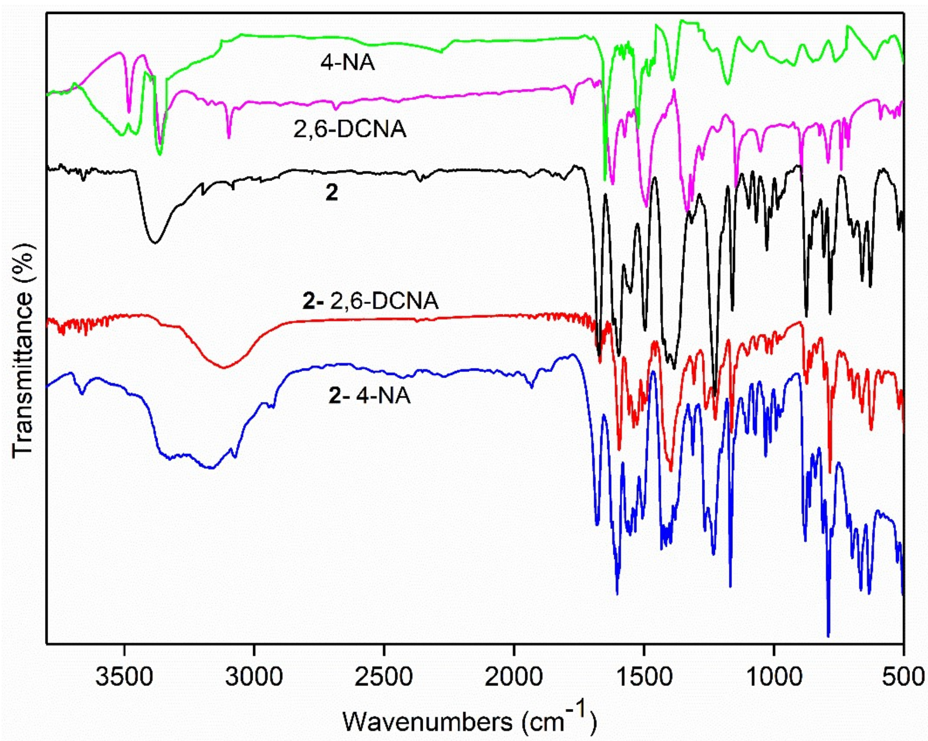

(b)

Fig. S25 UV-vis absorption spectrum of 4-NA and 2,6-DCNA in DCM solution and the excitation and emission spectra of (a) **1** and (b) **2**.

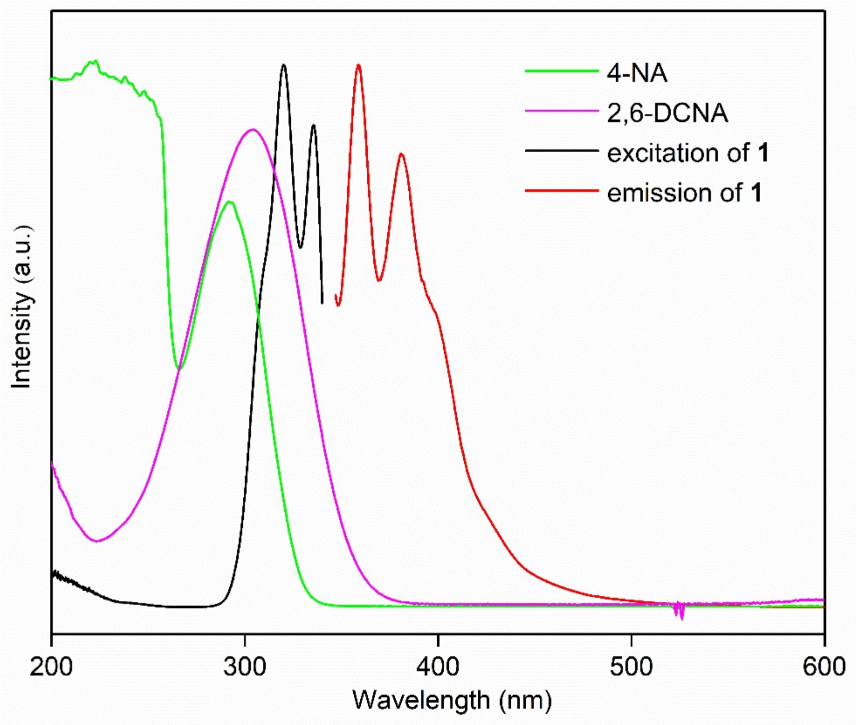

(a)

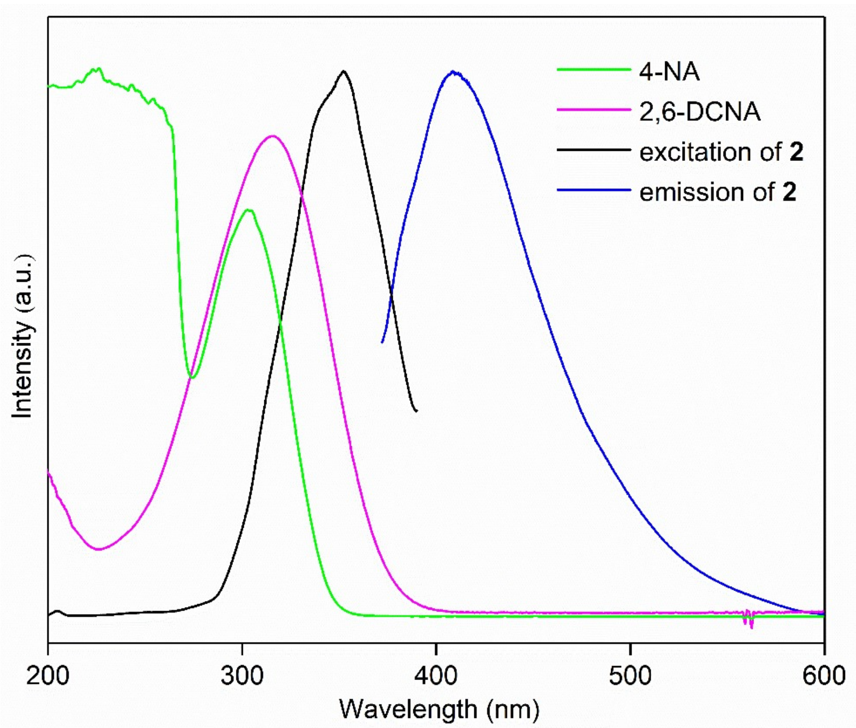

(b)

Fig. S26 Water contact angle (WCA) images of samples (a) **1** (b) **2** (c) **3** (d) **4** (e) **5** and (f) **6**

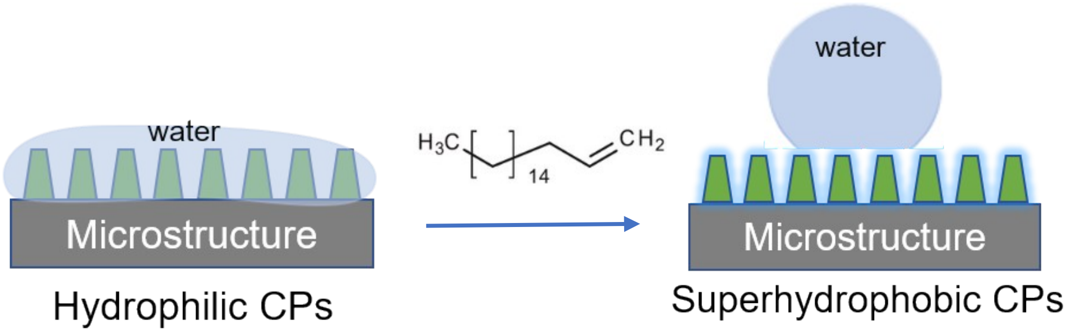

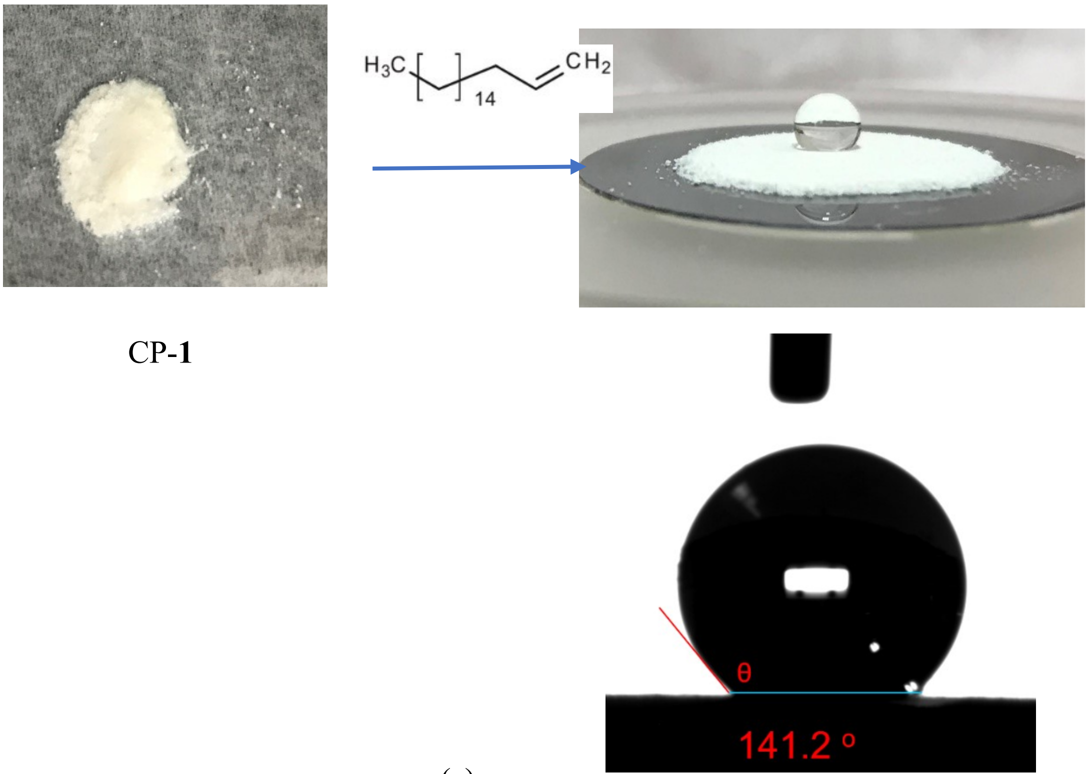

CP-**1**

(a)

CP-**1**-C-18

CP-**2**

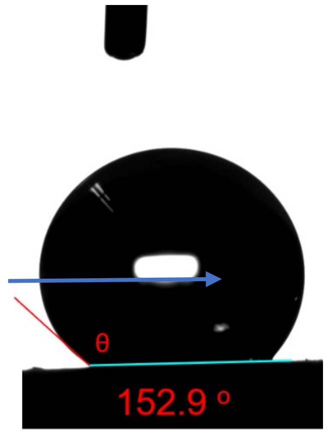

CP-**2**-C-18

(b)

CP-**3**

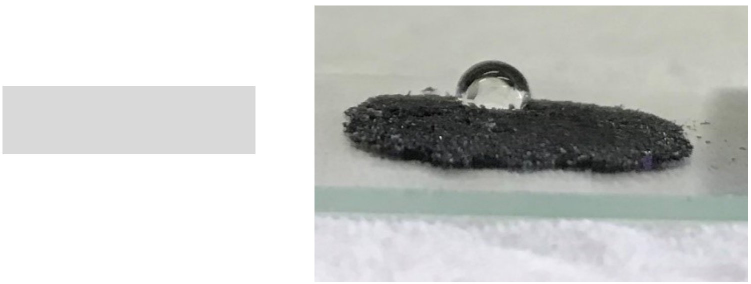

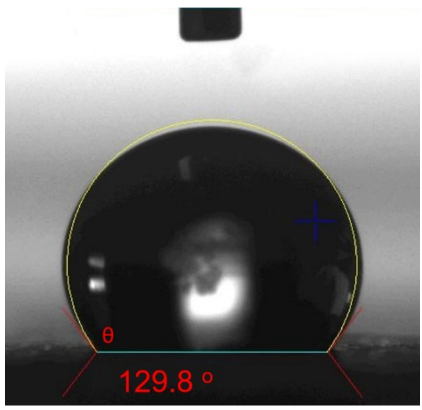

CP-**3**-C-18

(c)

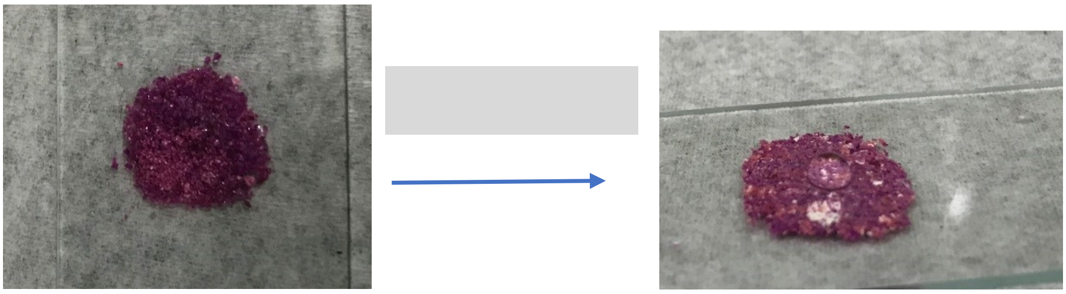

CP-**4**

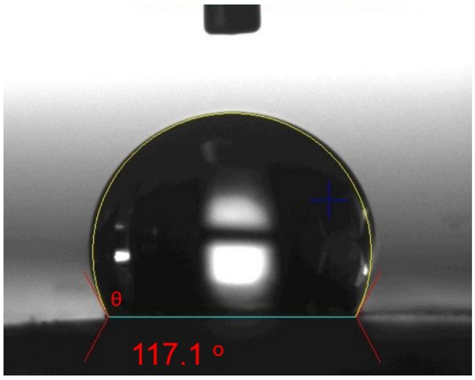

CP-**4**-C-18

(d)

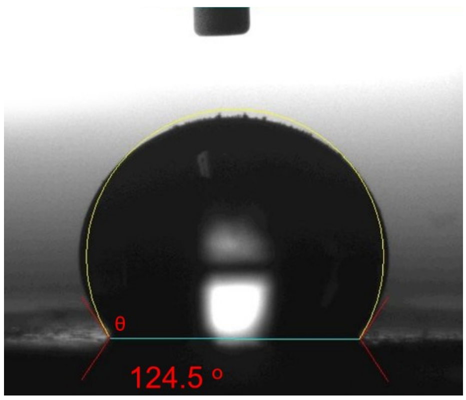

CP-**5**

CP-**5-**C-18

(e)

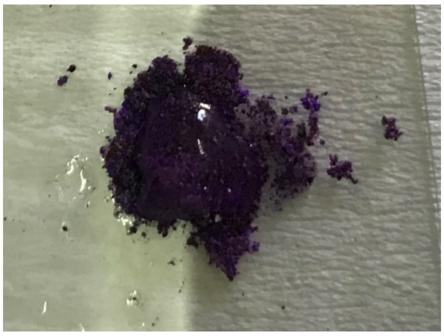

CP-**6-**C-18

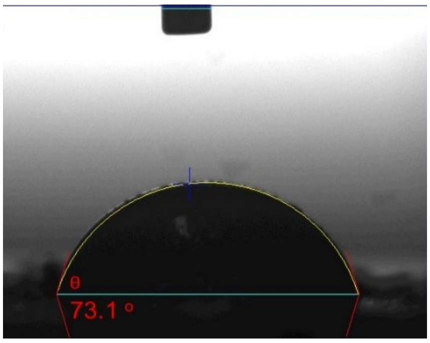

(f)

Fig. S27 FT-IR analysis for **2** (black curve) and **2**-C18 (red curve).

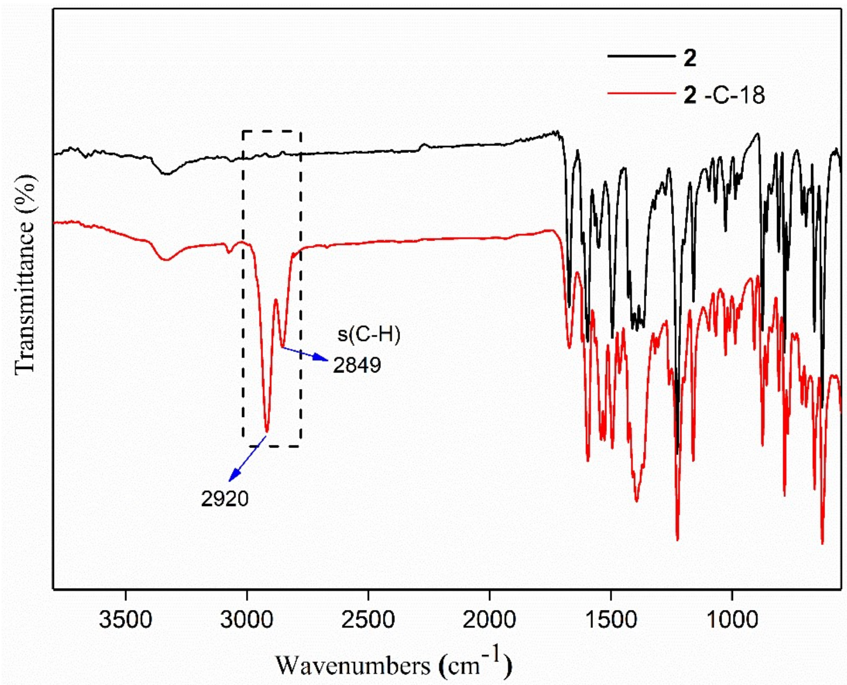

Fig. S28 TGA curves for activated **2a** (black) and **2a**-C18 (red).

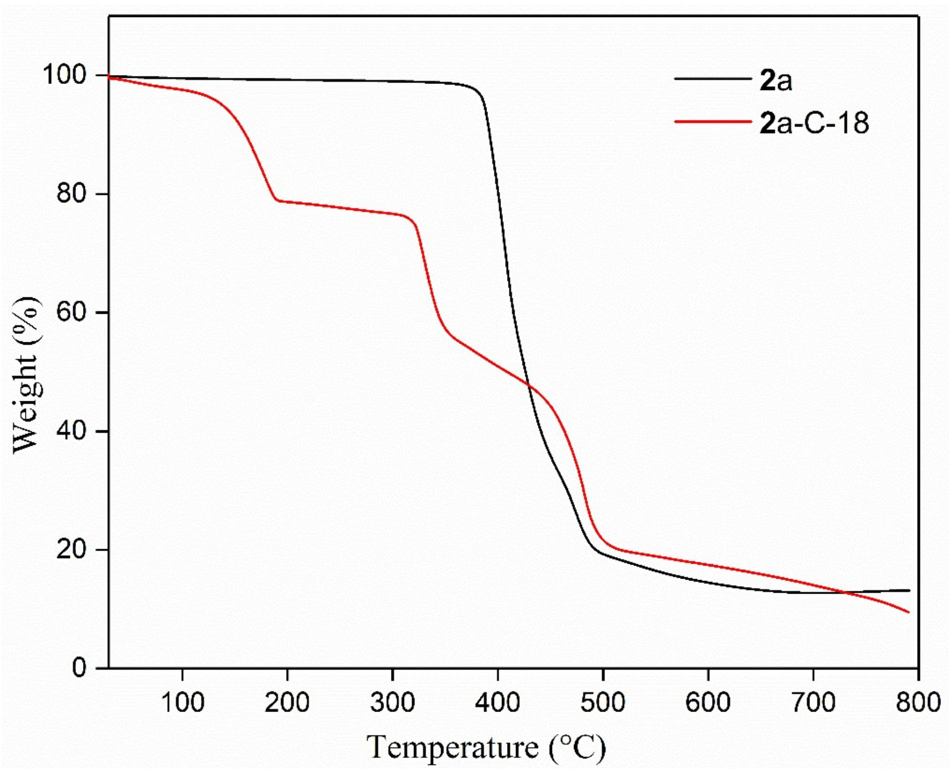

Fig. S29 (a) CO_2 uptake at 273 K for **2a** and **2a**-C18. (b) SEM images of **2** before and after post-synthesis modification.

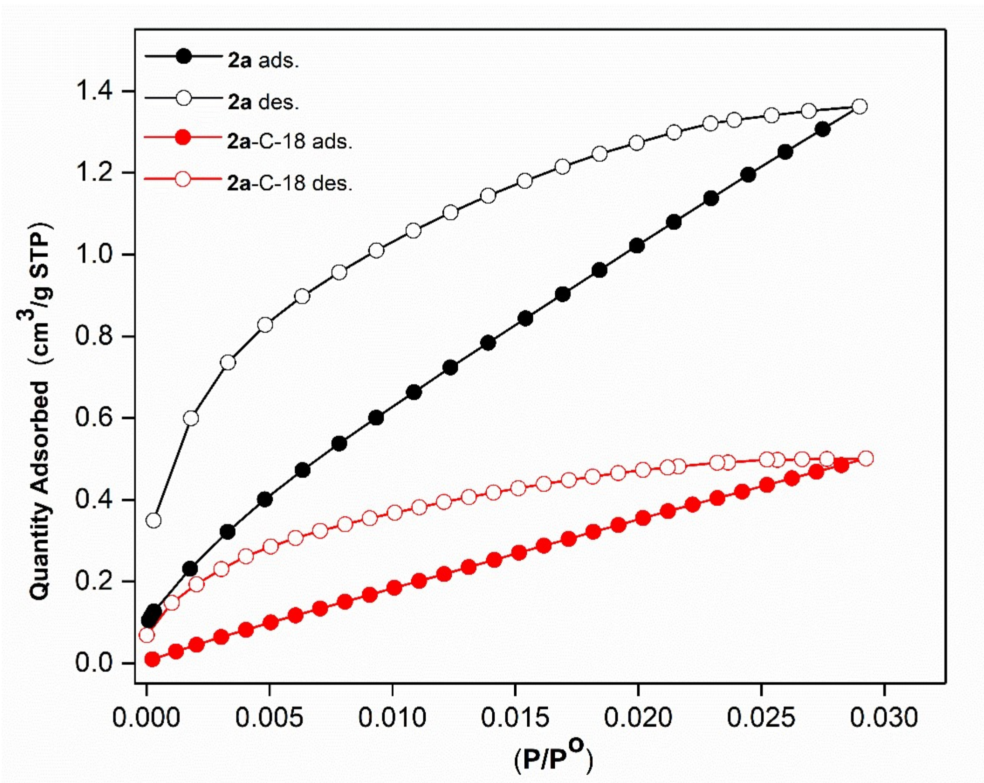

(a)

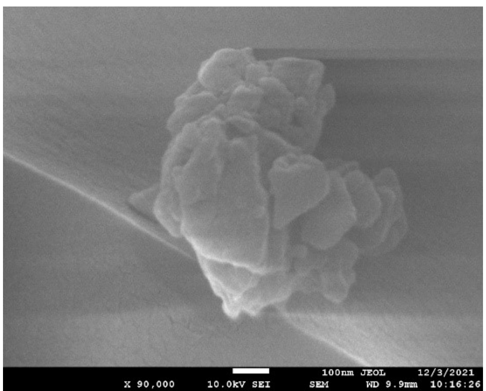

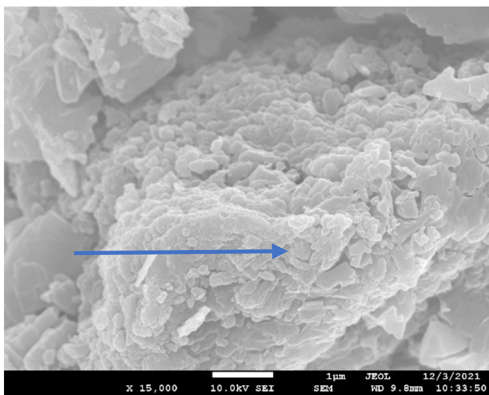

PSM

2 **2-**C-18

(b)

Table S1. Sensing properties of reported compounds towards 2,6-DCNA, and 4-NA pesticides.

Complex	Analytes	Stern-Volmer constant (K_{sv}, M^{-1})	Adjusted R^2	Limit of detection (μM)	Reference
$\{[Zn(\mathbf{L^1})_{0.5}(FIPBB)\cdot H_2O]\}_n$, **1**	2,6-DCNA, 4-NA	1.136×10^4 1.313×10^4	0.981 0.992	3.62 4.14	this work
$\{[Zn(\mathbf{L^2})(OBA)\cdot CH_3OH]\}_n$,**2**	2,6-DCNA, 4-NA	2.025×10^5 2.623×10^5	0.988 0.992	2.86 1.94	this work
Mg-APDA	2,6-DCNA	7.50×10^4	0.9815	1.50	*Inorg. Chem.* 2018, 57, *21*, 13330–13340.
$[\{Zn(L)_2(DMF)_4\} \cdot 2BF_4]_\alpha$ $[\{Cd(L)_2(Cl)_2\} \cdot 2H_2O]_\alpha$	2,6-DNA, 4-NA	6.401×10^4 7.130×10^4	0.995 0.919	2.97 0.90	Chem Asian. J. 2022, *17*, 202101204.
$(H_3O)[Zn_2L(H_2O)]\cdot 3NMP\cdot 6H_2O$	2,6-DCNA	6.072×10^3	0.922	5.4	RSC Adv**.**, 2019, *9*, 38469-38476.
$[Eu_2(dtztp)(OH)_2(DMF)(H_2O)_{2.5}]\cdot 2H_2O$	2,6-DCNA	6.25×10^4	0.995	2.91	Sensors and Actuators: B. Chemical, 2021, *331*, 129377.
$[Ag(3\text{-}dpyb)(H_3odpa)]\cdot H_2O$	2,6-DCNA	2.028×10^5	0.988	1.15	RSC Adv., 2020, *10*, 44712–44718.
$\{[Cd(tptc)_{0.5}(bpz)(H_2O)]\cdot_{0.5}H_2O\}_n$ $[Cd(tptc)_{0.5}(bpy)]_n$	2,6-DCNA 2,6-DCNA	4.71×10^4 8.27×10^3	0.989 0.994	1.14 6.38	Molecular and Biomolecular Spectroscopy, 2020, *239,* 118467.
$[Zn_2(bpdc)_2(BPyTPE)]$	2,6-DCNA	8.04×10^3	0.996	1.30	Chem. Commun., 2017, *53*, 9975-9978.
$[Cd_3(L^2)_2(H2O)4]\cdot 5H_2O$ (4)	4-NA	2.15×10^4	0.998	1.14	Cryst. Growth Des. 2018, 18, 431−440.
$[Cd(ppvppa)(1,4\text{-}NDC)]_n$ (10)	4-NA	1.3×10^3	0.985	1.20	Cryst. Growth Des. 2015, 15, 2753–2760.
$[Cd(tptc)_{0.5}(phen)]$	2,6-DCNA	5.18×10^4		1.02	New J. Chem., 2019, 43, 13349-13356.
$[Zn_3(DDB)(DPE)]$	2,6-DCNA	3.3×10^4	0.990	3.3	Dalton Trans., 2019, 48, 16776-16785.
LNU-45 LNU-47	2,6-DCNA 2,6-DCNA	9.09×10^4 1.62×10^3	0.998 0.992	1.5 1.9	Molecules, 2022, *27*, 126.